

https://dspace.org/

Time-dependent seismic hazard in mining.

Finnie, Gerard John.

1993
https://hdl.handle.net/10539/24505

Downloaded from a DSpace repository. https://dspace.org/

TIME-DEPENDENT SEISMIC HAZARD IN MINING

Gerard John Finnie

A project report submitted to the Faculty of Mining Engineering, University of the Witwatersrand, Johannesburg, in partial fulfilment of the requirements for the degree of Master of Science in Engineering.

CARLETONVILLE, 1993

DECLARATION

I, GERARD JOHN FINNIE, hereby declare that this project report is my own work and has not been previously submitted as a project peport, dissertation or thesis for any degree at any other University.

(Signature of candidate) 

20th day of OCTOBER 1993

ABSTRACT

A strategy to determine the probability that a mining induced seismic event will occur with magnitude which exceeds some specified value within a given time is investigated.

The model allows for a non-linear frequency-magnitude relationship and a Poissonian distribution of seismic events in time. The procedure is also independent of the method of mining and of the mining geometry.

The model was applied to clusters of various sizes, starting from small areas on a single reef and ending up with the entire mine as a single entity.

It was shown that the model works well with large populations of events, but to be successful with small clusters, the retention of the Poisson distribution is too restrictive and a non-stationary model of seismic event occurrence in time will have to be developed.

ACKNOWLEDGMENTS

Thanks and sincere appreciation are directed to the following persons and institutions:

- My supervisors, Dr I. Clark, Faculty of Mining Engineering, University of the Witwatersrand, and Dr R.W.E. Green, Bernard Price Institute of Geophysics, University of the Witwatersrand, for their help and guidance.

- Professor Andrzej Kijko, who introduced me to this line of research in the first place, and who has helped me with the theoretical aspects of the project.

- Mr A. van Zyl Brink, for his help with the specification and operation of the ISS network.

- Mr K.L. Riemer, for his support and interest in this project.

- ISS International, for allowing me to use their offices, equipment and data.

- Goldfields of South Africa for granting me study leave and assisting me financially.

CONTENTS

		Page
DECLARATION		ii
ABSTRACT		iii
ACKNOWLEDGMENTS		iv
LIST OF FIGURES		vi
LIST OF TABLES		ix
INTRODUCTION		1
CHAPTER 1	Specification of the Equipment	3
CHAPTER 2	Theoretical Background	6
CHAPTER 3	Results	21
CHAPTER 4	Discussion and Conclusion	60
APPENDIX A	Magnitude	66
APPENDIX B	Sufficiency Conditions for Maxima	72
APPENDIX C	The Poisson Process	75
APPENDIX D	Space-Time Clustering	76
APPENDIX E	Program Listings	79
APPENDIX F	Fragment of the Data	94
APPENDIX G	Correlation between Seismicity in Adjacent Areas	95
REFERENCES		96

LIST OF FIGURES

Figure		Page
2.1	Frequency-magnitude histogram	6
2.2	Frequency-magnitude relationship	7
2.3	Graphing Eq. (2.2) for various values of C	8
2.4	Weibull probability density function	11
2.5	Weibull cumulative distribution function	11
2.6	Crossection through reefs	16
2.7	Scheme for the evaluation of the time-dependent seismic hazard	19
3.1	Increase in activity rate due to physical reasons	34
3.2	Increase in activity rate due to improved instrumentation	34
3.3	Scatter diagram for the VCR events	37
3.4	Scatter diagram for the CLR events	38
3.5	Scatter diagram of events in the Y-Z plane	39
3.6	Selected clusters on the VCR	40
3.7	The effect of blasting on activity rate	41
3.8	Seismic hazard for cluster 1 on the VCR for various parameter windows	42
3.9	Seismic hazard for cluster 1 on the VCR : zoomed in for days 300-470	43
3.10	Frequency-magnitude relationships for both reefs	44
3.11	Large events on the VCR and CLR	45
3.12	Seismic hazard for the VCR and CLR	46

Figure		Page
3.13	Gutenberg-Richter relationship for the entire mine	47
3.14	Activity rates for the entire mine	48
3.15	Events with magnitude ≥ 15.50 for the entire mine	49
3.16	Events with magnitude ≥ 16.00 for the entire mine	50
3.17	Events with magnitude ≥ 16.25 for the entire mine	51
3.18	Values of β, C and N in each parameter window (entire mine) parameter window = 12 days, prediction magnitude = 15.50 prediction window = 7 days	52
3.19	Values of β, C and N in each parameter window (entire mine) parameter window = 30 days, prediction magnitude = 16.00 prediction window = 20 days	53
3.20	Values of β, C and N in each parameter window (entire mine) parameter window = 45 days, prediction magnitude = 16.25 prediction window = 43 days	54
3.21	Seismic hazard (entire mine) : parameter window = 12 days prediction magnitude = 15.50, prediction window = 7 days	55
3.22	Seismic hazard (entire mine) : parameter window = 30 days prediction magnitude = 16.00, prediction window = 20 days	56
3.23	Seismic hazard (entire mine) : parameter window = 45 days prediction magnitude = 16.25, prediction window = 43 days	57
3.24	Seismic hazard (entire mine) - no "event arrows"	58
3.25	Time-magnitude relationship	59
4.1	The effect of too short a parameter window	63
4.2	A matched window-magnitude pair (right) contrasted with too long a parameter window (left)	65

Figure		Page
A1	One of three components of a typical velocity seismogram	66
A2	Displacement spectral density of the seismogram shown in Fig. (A1)	68
B1	Mesh of (the logarithm of) the likelihood function for typical values of the parameters	74

LIST OF TABLES

Table		Page
3.1	Particulars regarding cluster 1 on the VCR	23
3.2	Particulars regarding cluster 2 on the VCR	23
3.3	Particulars regarding cluster 3 on the VCR	24
3.4	Particulars of cluster 1 (VCR) after restrictions	25
3.5	Particulars of cluster 2 (VCR) after restrictions	25
3.6	Particulars of cluster 3 (VCR) after restrictions	26
3.7	Particulars regarding the entire VCR	28
3.8	Particulars regarding the entire CLR	29
3.9	Particulars of the entire VCR after restrictions	29
3.10	Particulars of the entire CLR after restrictions	30
3.11	Particulars regarding the entire mine	32
3.12	Particulars regarding the entire mine after restrictions	32
E1	Conversion from magnitude (x) to moment magnitude (M_L)	71
F1	A fragment of mining-induced seismic data	94
G1	X, Y coordinates of 4 analyzed clusters of seismic events	95
G2	Maximum cross-correlation coefficients	95

Introduction

ISS International has developed a methodology to assess the seismic hazard of a mining operation, which is independent of both the mining geometry and the method of mining. Prof. A. Kijko was responsible for the theoretical aspects of this project and Mr C.W. Funk originally wrote the computer program to implement this mine specific methodology using space-time clustering techniques (see Appendix D).

Because we are going to use a simplified approach to clustering, viz. visual identification of spatial clusters, it was felt that all computer programs should be re-written for this project specifically. This approach also has the advantage of flexibility, customization and independence during the research and validation phase of the methodology.

Typically the procedure starts by recording on a computer database, the totality of seismic events on a mine, (or a sufficiently large area of a mine), over a sufficiently long period of time - typically years - using a reasonably high resolution seismic network. The concepts loosely described here will be made concrete in Chapter 2.

We believe that seismic information can be gleaned, not from the average seismicity prevailing over the entire mine, but from the anomalous behaviour of seismicity. On account of this, the first phase of the program scans the entire database and clusters of seismicity are identified manually. All subsequent statistical analysis is then performed on these clusters separately, the clusters being regarded as independent populations or catalogues of events.

Having selected a particular cluster, the cumulative frequency-magnitude diagram is drawn for the entire span of the catalogue. From this one is able to determine

the threshold of completeness of the catalogue, events of magnitude less than this threshold being discarded.

During the operation of the second phase of the program, estimates of the parameters defining the time-dependent seismic hazard are obtained from a statistical analysis of the events in a moving time-window defined on the interval $(t-\Delta t', t]$ say, and this function is then used to find the probability of obtaining an event having magnitude equal or greater than x_M within the following time interval $(t, t+\Delta t]$. As these time windows increment their way chronologically through the catalogue, the corresponding probabilities are evaluated. The computer displays the results as a continuous function.

At this point in time, no thorough investigation has been made to determine the optimal values and relationships between certain parameters of the model e.g. prediction magnitudes and time-window durations etc., as well as the question of cluster size, which is important in view of a report (Kijko, 1993) which shows significant correlation of seismicity between adjacent mining areas.

This project report proposes to address the above issues.

Chapter 1

DESCRIPTION AND SPECIFICATION OF THE DATA ACQUISITION SYSTEM

Only those aspects of the system that pertain directly to the quality of the data and to the processing of seismic parameters used in this project, will be dealt with in this chapter.

General Description

All data for this project was collected and processed by the **Integrated Seismic System.** The ISS, as it is known, is comprised of remote stations, a communication system and a central computer. It is Digital, Intelligent and performs on-line Automatic, Quality Controlled, Seismological processing. In our case, the remote stations happen to be *Intelligent Seismometers.*

An Intelligent Seismometer:

- calibrates and monitors a triaxial set of geophones
- keeps network time
- triggers on seismic events
- describes all triggered events to the central computer in terms of time, amplitude and duration
- sends waveforms on request
- keeps largest events if triggers are faster than transmission

Seismological processing produces the following results

Ground Motion Characteristics

- average background noise level
- maximum amplitude and period
- central 90% of energy experienced by a given station (E90) and its duration (T90)
- power of the ground motion = E90/T90
- spectral parameters

Location

- P and S arrivals
- direction, azimuth and take-off angle
- X,Y,Z - coordinates of the hypocentre
- location error estimates

Seismic Moment Tensor

- decomposition into isotropic and deviatoric components
- directions of principal stresses acting at the source and fault plane solution
- radiation pattern

Source Parameters

- seismic moment
- radiated energy
- corner frequency
- static and dynamic stress drop
- magnitude

The advantage of a digital system lies primarily in maintaining the integrity of acquired seismological data. With conversion to a digital format as close as possible to the sensors, maximum dynamic range can be ensured. Accurate calibration of the seismic waveform data is easy to maintain. Digital communication between the remote sites and a central computer allows for transmission of waveforms with no amplitude or phase distortion.

For every seismic event of $M_L \geq 3$ there can be over 10 000 events with $M_L \geq -1$. To get reliable source parameters, every event should be recorded by at least 5 three-component stations surrounding the source, giving a total of 150 000 waveforms to be processed. This cannot be done manually, and the ISS resorts to quality controlled, automatic processing, and the operator interacts only when required.

Specification

Intelligent Seismometer

Dynamic range	132 dB
A/D resolution	12 bits
Sampling rate per component	2 kHz
Anti-aliasing onset	500 Hz
Filter	6 th. order Bessel
Geophone	4.5 Hz resonance frequency
Real time clock resolution	500 μs
Communication channel	Modem

System

Sensors	triaxial geophones in 20m boreholes
Configuration	26 sensors 1.5km ave. source to sensor distance
Sensitivity	M_L(min) < -0.5
Min. velocity for triggering	1×10^{-5} m/s
Location process	L_1 - norm
Mean location error	50m
Sensor lattice dimensions	8km x 3km x 3.5km (L x W x D)

Chapter 2

THEORETICAL BACKGROUND

PART I

Let the sample space Ω be the totality of events ω_i $(i = 1, 2, \ldots, n)$, recorded in a particular region of the mine over a given period of time by some given monitoring equipment.

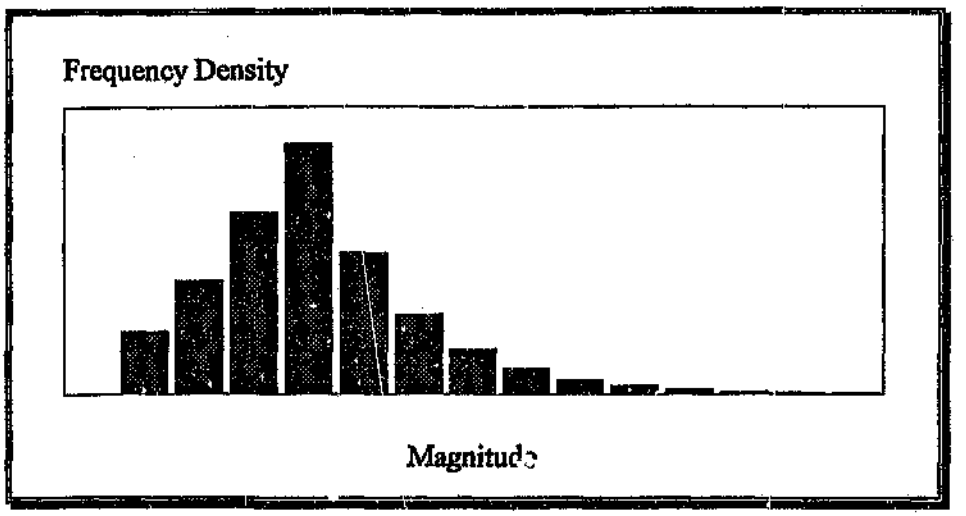


Figure 2.1 Frequency - magnitude histogram

Let us define a continuous random variable $X(\cdot)$ which associates with each event, some or other seismic parameter x, which in this case we take to be $\log (M_0 + \gamma E)$ and which we here call *magnitude*: M_0 is the seismic moment, E the seismic event energy and γ is a constant. See Appendix A.

If grouped magnitude is plotted in the form of a frequency density histogram, one obtains the general shape depicted in Figure 2.1.

Perhaps a more informative presentation of the data would be to plot the logarithm of the *cumulative frequency* against the magnitude; the upper curve in Figure 2.2. below.

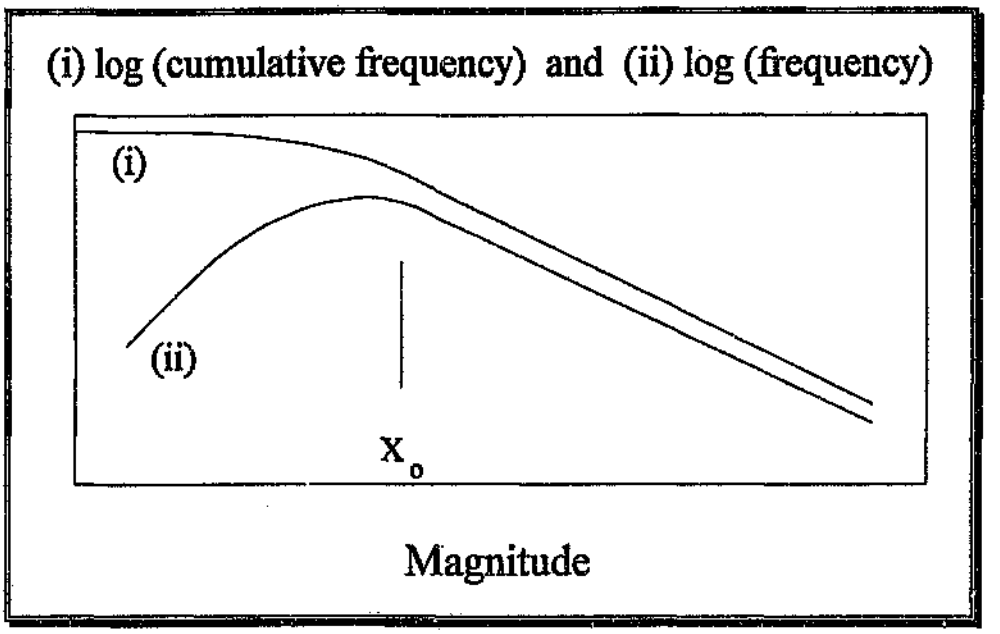


Figure 2.2 Frequency-magnitude relationships

This gives rise to the well known Gutenberg-Richter relationship $\log n(x) = a - bx$, where $n(x)$ is the number of events not less than magnitude x, a is the ordinate intercept of the linear portion of the graph produced, and b is the absolute value of the slope of this linear portion; the so-called *b-value*. If however, we let $n(x)$ represent the number of events in a given class interval about x, we get the lower curve in the Figure 2.2 above.

Of vital importance here is the identification of the magnitude x_0 above which the data set is *complete*. The "flattening" of the curve to the left of x_0 does not mean that the number of events with magnitude less than this are diminishing; rather it reflects the inadequacy of the monitoring equipment to register fully all events below this threshold value. In the analysis that follows, all events with magnitude

less than x_0 are discarded from the sample space Ω and we therefore work with a complete, albeit left-truncated set $\Omega_0 \subset \Omega$.

Bearing this in mind, it suits our purposes to re-write the Gutenberg-Richter relationship in the point-slope form, where α say, is the ordinate value corresponding to the threshold magnitude x_0, and also to change to Napierian logarithms, giving

$$\ln n(x) = \begin{cases} 0 & x < x_0 \\ \alpha - \beta (x - x_0) & x \geq x_0 \end{cases} \qquad (2.1)$$

with $\alpha = (a - bx_0) \ln (10)$ and $\beta = b \ln (10)$.

Unfortunately, when actual data from a cluster, belonging to the set Ω_0, from the mining environment, is plotted according to the above scheme, it is observed that the graph is not a straight line, but somewhat curved. This means that equation (2.1) has to be generalized to accommodate this and Cornell and Winterstein., (1988) have suggested

$$\ln n(x) = \begin{cases} 0 & x < x_0 \\ \alpha - \beta (x - x_0)^C & x \geq x_0 \end{cases} \quad ; C \geq 1 \qquad (2.2)$$

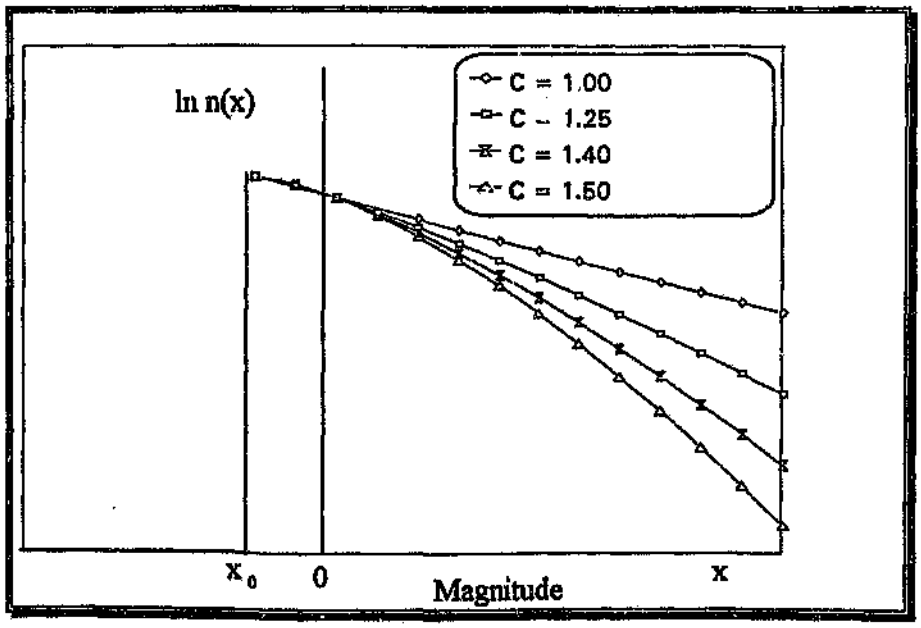


Figure 2.3 Graphing Equation (2.2) for various values of C

Equation (2.2) can be re-written as

$$n(x) = \begin{cases} 0 & x < x_0 \\ \exp[\alpha - \beta(x-x_0)^C] & x \geq x_0 \end{cases}$$

Let us write

$$f(x) = \frac{dn(x)}{dx} = \begin{cases} 0 & x < x_0 \\ -\beta C(x-x_0)^{C-1} \exp[\alpha - \beta(x-x_0)^C] & x \geq x_0 \end{cases} \qquad (2.3)$$

In order for $f(x)$ to qualify as a probability density, it must satisfy

i) $f(x) \geq 0 \quad \forall x \in R$

ii) $\int_{-\infty}^{\infty} f(x)dx = 1$

Condition (i) requires that we drop the leading negative sign because all factors to the right of it are positive, and condition (ii) forces

$$\int_{x_0}^{\infty} \beta C(x-x_0)^{C-1} e^{\alpha - \beta(x-x_0)^C} dx = -e^{\alpha - \beta(x-x_0)^{C-1}} \Big|_{x_0}^{\infty} = e^{\alpha} = 1 \Rightarrow \alpha = 0$$

Hence, the probability density function is

$$f_X(x) = \begin{cases} 0 & x < x_0 \\ \beta C(x-x_0)^{C-1} \exp[-\beta(x-x_0)^C & x \geq x_0 \end{cases} \qquad (2.4)$$

The *cumulative distribution function* can be obtained from the probability density function according to $F_X(x) = \int_{-\infty}^{x} f_X(u)du$. Hence, from equation (2.4),

$$F_X(x) = \begin{cases} 0 & \\ \int_{x_0}^{x} \beta C(u-x_0)^{C-1} \exp[-\beta(u-x_0)^C]\,du & \end{cases} = \begin{cases} 0 & x < x_0 \\ 1-\exp[-\beta(x-x_0)^C] & x \geq x_0 \end{cases}$$

(2.5)

Equations (2.4) and (2.5) are known as the *Weibull distribution functions* (e.g. Johnson and Kotz, 1970) and are often used in modelling seismic event occurrences (Utsu, 1984; Cornell and Winterstein, 1988)

If $C = 1$, the formulas reduce to the *exponential distribution functions* (e.g. Johnson and Kotz, 1970).

$$f_X(x) = \begin{cases} 0 & x < x_0 \\ \beta \exp[-\beta(x-x_0)] & x \geq x_0 \end{cases} \qquad (2.6)$$

$$F_X(x) = \begin{cases} 0 & x < x_0 \\ 1-\exp[-\beta(x-x_0)] & x \geq x_0 \end{cases} \qquad (2.7)$$

Figure 2.4. and Figure 2.5. below, show the graphs of equation (2.4) and equation (2.5) respectively, for typical values of the parameters β and C, and threshold magnitude x_0.

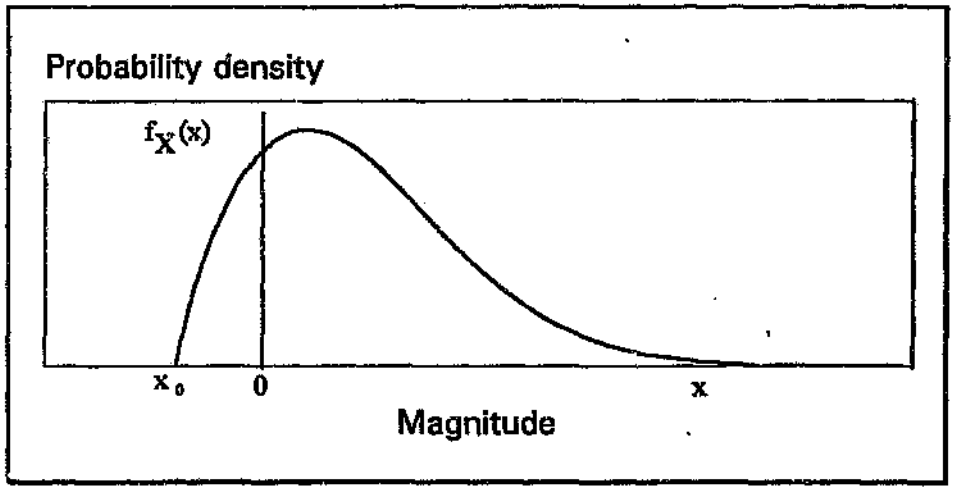


Figure 2.4 Weibull probability density function

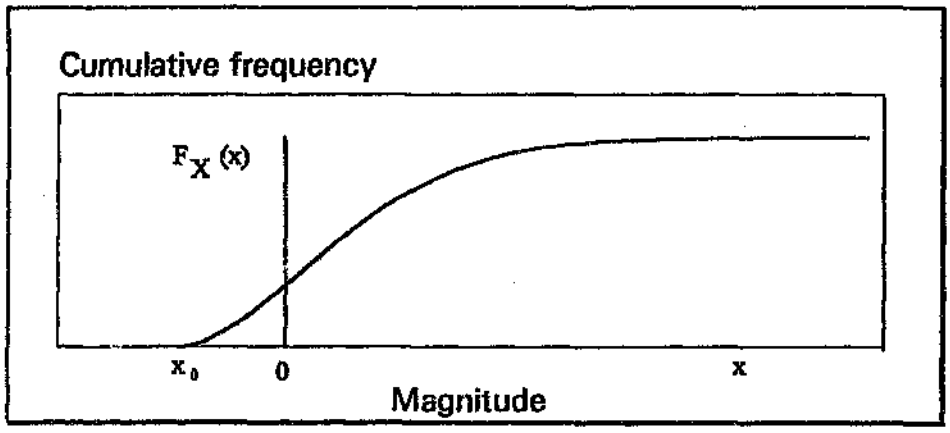


Figure 2.5 Weibull cumulative distribution function

Of all the methods available to us for the estimation of parameters, only two have been used extensively to estimate b, viz. the *method of least squares* and the *method of maximum likelihood.*

The least squares method tends to estimate too low a *b*-value, because it cannot include magnitudes above the maximum observed. (Bender, 1983). Therefore, in keeping with most authors today, we are going to find the maximum likelihood estimators of β and C.

The Maximum Likelihood Estimators of β and C

Let ω_i be n observed events in Ω_0 with corresponding magnitudes x_i i.e. let $X(\omega_i) = x_i \quad (i = 1, \ldots, n)$. Then the *likelihood function* is given by

$$L(\beta,C) = \prod_{i=1}^{n} \beta C(x_i - x_0)^{C-1} \exp[-\beta(x_i - x_0)^C] \tag{2.8}$$

The *maximum likelihood estimators* of β and C are those values of these parameters which maximize $L(\beta, C)$.

Therefore, to find the maximum likelihood estimate of β we differentiate Eq. (2.8) partially with respect to β, and equate to zero. Fortunately, the result is equivalent to first taking logarithms on both sides of Eq. (2.8) and then proceeding to differentiate and equate to zero.

$$\ln L(\beta,C) = n\ln\beta + n\ln C + (C-1)\sum_{i=1}^{n}\ln(x_i - x_0) - \beta\sum_{i=1}^{n}(x_i - x_0)^C$$

$$\frac{\partial \ln L(\beta,C)}{\partial\beta} = \frac{n}{\beta} - \sum_{i=1}^{n}(x_i - x_0)^C \qquad \text{and}$$

$$\frac{\partial \ln L(\beta,C)}{\partial\beta} = 0 \Rightarrow \beta = \left[\frac{1}{n}\sum_{i=1}^{n}(x_i - x_0)^C\right]^{-1} \tag{2.9}$$

To obtain the maximum likelihood estimate of C, we proceed as before except that now we differentiate partially with respect to C.

$$\frac{\partial \ln L(\beta,C)}{\partial C} = \frac{n}{C} + \sum_{i=1}^{n}\ln(x_i - x_0) - \beta\sum_{i=1}^{n}(x_i - x_0)^C \ln(x_i - x_0)$$

Using Eq. (2.9) to substitute for β and equating the result to zero gives rise to

$$\frac{1}{C} + \frac{1}{n}\sum_{i=1}^{n}\ln(x_i - x_0) = \left[\frac{1}{n}\sum_{i=1}^{n}(x_i - x_0)^C\right]^{-1}\frac{1}{n}\sum_{i=1}^{n}(x_i - x_0)^C \ln(x_i - x_0) \tag{2.10}$$

Equations (2.9) and (2.10) can be more conveniently written

$$\beta = \frac{1}{\left\langle (x-x_0)^C \right\rangle} \quad \text{and} \tag{2.9a}$$

$$\frac{1}{C} + \left\langle \ln(x-x_0) \right\rangle = \frac{\left\langle (x-x_0)^C \ln(x-x_0) \right\rangle}{\left\langle (x-x_0)^C \right\rangle} \tag{2.10a}$$

were $\langle \cdot \rangle$ represents the average over the samples.

Simultaneous solutions of Equations (2.9) and (2.10) give rise to the required maximum likelihood estimators $\hat{\beta}$ and $\hat{C}$ of β and C respectively.

In the special case where $C = 1$ (classical Gutenberg-Richter relationship), Equation (2.9) takes on a particularly simple form. (Aki, 1965; Utsu, 1965).

$$\hat{\beta} = \left[\frac{1}{n} \sum_{i=1}^{n} (x_i - x_0) \right]^{-1} = \frac{1}{\frac{1}{n}\left[\sum x_i - n x_0 \right]} = \frac{1}{\langle x \rangle - x_0} \tag{2.11}$$

[It is to be noted that Equations (2.9) and (2.10) are *necessary* but not *sufficient* conditions for the maximizing of Equation (2.8). See Appendix B].

From the central limit theorem it follows that for sufficiently large n, $\hat{\beta}$ is approximately normally distributed about its mean value given by (2.11) [1], with standard deviation equal to (Eadie, et al., 1982)

$$\hat{\sigma}_\beta = -\left(\frac{\partial^2 \ln L}{\partial \beta^2} \right)^{-\frac{1}{2}}_{\hat{\beta}} = \frac{\hat{\beta}}{\sqrt{n}}$$

and since $b = \beta \log(e)$, the standard deviation of $\hat{b}$ is $\hat{\sigma}_b = \frac{\hat{\beta} \log(e)}{\sqrt{n}}$.

[1] For large n, C tends to be close to 1.

The probability rate of occurrence of seismic events λ

The activity rate, as its generally known, is given by $\lambda = n/\Delta t'$, where n is the total number of events with magnitudes greater than or equal to the threshold magnitude, and $\Delta t'$ is the time span over which these events occurred.

Assuming $\Delta t'$ is such that the occurrence of events in the time interval $(t-\Delta t', t]$ follows a Poisson distribution, and that $\Delta t'$ is long enough to obtain sufficient data for a reliable estimation of the parameters, the probability of at least one seismic event with $x \geq x_0$, occurring between t and $t + \Delta t$ is

$$1 - \exp(-\lambda \Delta t). \qquad (2.12)$$

(See Appendix C for details).

Seismic Hazard

By *seismic hazard* we mean the probability of obtaining a seismic event of magnitude x, greater than some given magnitude x_M, which is above the threshold value x_0, within a given time interval $(t, t + \Delta t]$.

From equation (2.5), we see that the probability of getting an event less than x_0 is

$$P_r(x < x_0) = F(x_0) = 1 - \exp[-\beta(x_0 - x_0)] = 0$$

Hence, the probability of getting an event equal to or greater than x_0 is given by

$$P_r(x \geq x_0) = 1 - P_r(x < x_0) = 1$$

and for this situation, the activity rate is λ seismic events per unit time.

Therefore, the activity rate λ_M for the occurrence of events with magnitude $x \geq x_M$ where $x_M \geq x_0$, must be equal to λ times the probability of getting these larger events.

That is, $\lambda_M = \lambda[P_r(x \geq x_M)] = \lambda[1 - P_r(x < x_M)] = \lambda[1 - F(x_M)]$

From Equation (2.12), it follows that the seismic hazard, given by the probability of obtaining at least one event equal to or greater than x_M, during the interval $(t,\ t+\Delta t]$ is given by

$$1-\exp(-\lambda_M \Delta t) \qquad (2.13)$$

PART II

In this section we will show how to

(i) obtain the sets referred to above as Ω_0

(ii) impose time-dependency on the hazard function (2.13).

The computer programs used in this project are divided into two phases. (see Appendix E for program listings). The programs belonging to the first phase are used to filter the raw data and have as their objective the delineation of the clustering. The second phase programs operate only on selected clusters to produce statistical information.

First Phase (clustering)

Two gold-bearing reefs are mined, one called the *Ventersdorp Contact Reef* (VCR) and the other called the *Carbon Leader Reef* (CLR). Both reefs are essentially planar.

In a coordinate system with origin 6000 ft above mean sea level, and in which the positive X-axis points southwards, the positive Y-axis points westwards, and the positive Z-axis points downwards - thus giving rise to a dextral system - the VCR

has the equation 0.3259X - 0.1949Y - Z -15079 = 0 and the CLR has the equation 0.3670X - 0.0885Y - Z -10798 = 0 where X, Y and Z are in meters. (See listing of program E.1, Appendix E). The domain of interest is approximately $25000 < X < 30500$ and $-46000 < Y < -37000$.

Only those seismic events which have been located by 5 stations or more will be kept. This is to ensure that we have quality locations.

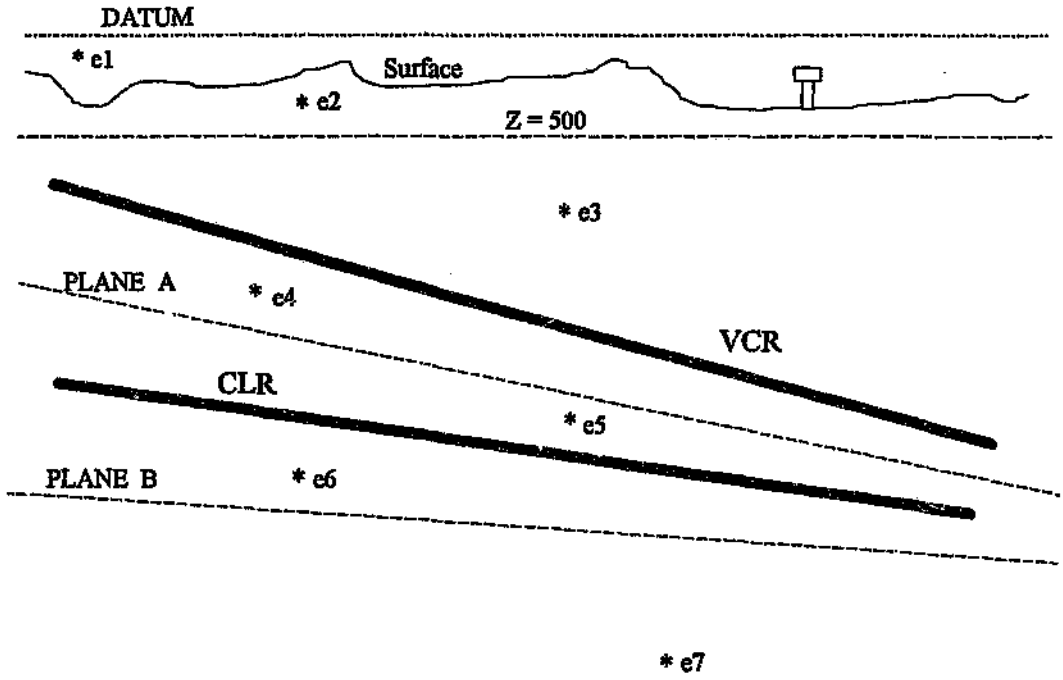


Figure 2.6 Crossection through the reefs

The Figure above shows an idealized crossection of the mine and is not to scale. It is idealized because the two reefs cannot be simultaneously edge on. However, it is sufficiently good for helping to explain the way in which the seismic events are going to be grouped.

Plane A bisects the vertical distance between the VCR and the CLR, and the CLR in turn, bisects the vertical distance between plane A and plane B.

Plane A and Plane B are defined in terms of the mine coordinate system as $0.34657X - 0.14175Y - Z - 12943.5 = 0$ and $0.3878X - 0.0353Y - Z - 8665.5 = 0$ respectively.

All the seismic events are now going to be classified in terms of their positions relative to three planes, i.e. in terms of their positions relative to plane A , plane B and the plane $Z - 500 = 0$.

- Events above the plane $Z - 500 = 0$ are simply going to be discarded, for it is unlikely to be a true event and is most likely the result of some corruption of previously good data. Examples of this are events e1 and e2.

- Events which lie below the plane $Z - 500 = 0$ and above plane A are going to be classified as those events falling under the influence of the VCR. Examples here are events e3 and e4.

- Events which lie between plane A and plane B are reckoned to be those which are most influenced by the mining on the CLR. Examples are events e5 and e6.

- Finally, those events which happen to be below plane B cannot easily said to be influenced by one or other of the reefs separately. An example here is event e7.

Note: there is little point in defining a plane similar to plane A e.g. above the VCR because there is a physical limit as to how shallow events can be, (they have to be below the surface e.g.), but no theoretical limit as to how deep in the earth's crust they can be. Also , events do not happen too high into the VCR hanging-wall anyway. Large, and very deep events are fault-plane slip type events, and can be initiated by mining either on the VCR or on the CLR, whereas events in the hanging-wall of the VCR are of various types but usually attributable to mining on the VCR itself. The plane $Z = 500$ is really superfluous - it's there just to guard against electronic corruption of the data e.g.

Figures (3.3), (3.4) and (3.6) on pages 37, 38 and 40 respectively, have all been obtained in accordance with this scheme.

Second Phase (time dependent hazard)

Before actually getting down to the main aspect of this section it is necessary to determine the threshold of completeness x_0, for each of the clusters. To achieve this, the cumulative frequency-magnitude diagram is drawn for each cluster and x_0 determined by inspection. Since we are dealing with an entire cluster, there are usually sufficiently many events for the diagram to at least approximate the classical Gutenberg-Richter relationship, and hence the cut-off point can most likely be recognised without too much trouble. It would be a good idea to confirm the results of the cutoff with activity rates in the cluster before and after cutoff, on account of the subjective nature of estimating x_0. The value of x_0 can change from place to place on the mine because (i) the density of geophones is not uniform throughout the mine, (ii) the rock quality, and hence the attenuation, changes from place to place, and (iii) different types of source mechanisms can predominate in different areas. Therefore, there can be a different threshold of completeness for each cluster.

Having discarded all events below the threshold, we have given practical expression to our theoretical set Ω_0.

Time Windows

We have two windows, a *parameter-window* and, immediately ahead of it, a *prediction-window*. The lengths of both these windows are controlled by the user. The parameter window operates only on complete data that belongs to a selected cluster.

The Parameter Window

As its name suggests, this window is used for the purpose of calculating the parameters C, β and λ of the hazard function (2.13), based on all the events in the window at any given time. As the window moves through the data chronologically, new events enter the window and old ones leave it. Therefore, the values of C, β and λ will change in time and so we must write $C = C(t)$, $\beta = \beta(t)$ and $\lambda = \lambda(t)$.

The Prediction Window

The parameters calculated in the parameter window are now assumed to be valid for the duration of the prediction window. In other words, the results of the parameter window are extrapolated to the prediction window where the hazard is then calculated and plotted.

The equation for calculating the time dependent seismic hazard can now be given

$$H(x_M|t) = P_r\{x \geq x_M|(t, t+\Delta t]\} = 1-\exp[-\lambda_M(t)\cdot\Delta t]$$

$$= 1-\exp\left\{-\lambda(t)\cdot\Delta t\ \exp\left[-\beta(t)(x_M - x_0)^{c(t)}\right]\right\} \qquad (2.14)$$

where x_M $(> x_0)$ is the so called *prediction level* or *prediction magnitude.*

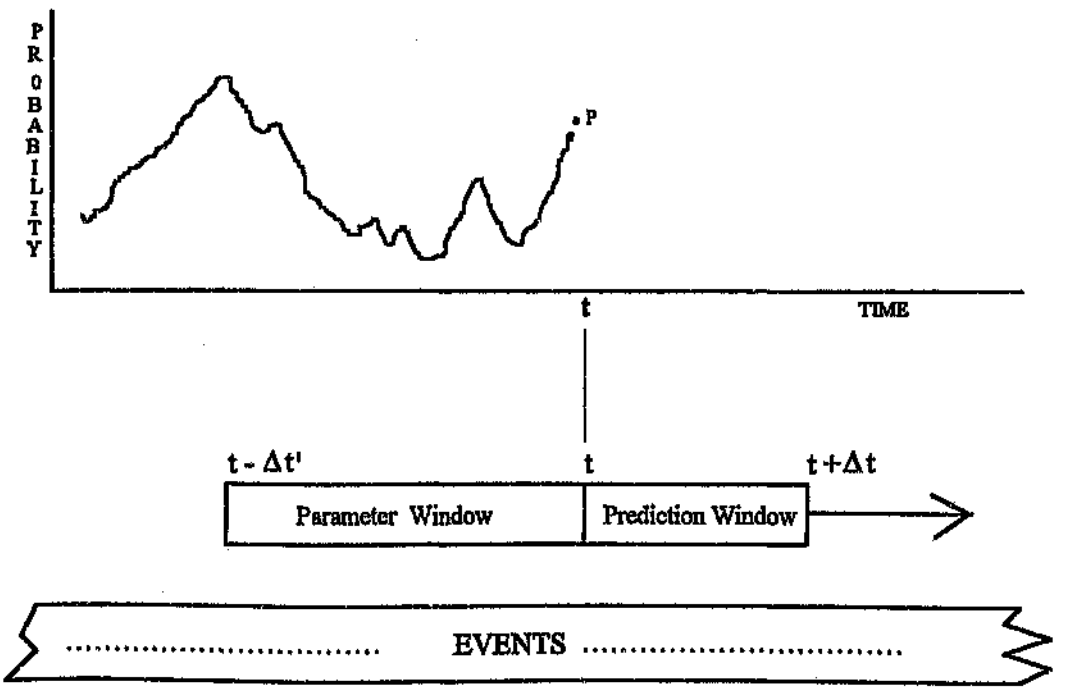


Figure 2.7 Scheme for the evaluation of the time-dependent seismic hazard

P is the probability of obtaining an event of magnitude $\geq x_M$ within the time interval $(t,\ t + \Delta t]$ based on an extrapolation of parameters calculated in the interval $(t - \Delta t',\ t]$.

Chapter 3

RESULTS

In this Chapter we will be presenting the methods that were followed and the results that were obtained of our model's interaction with the data. We must bear in mind that at a later stage we will want to answer the following questions or concepts.

(i) how does our model cope with clusters of various sizes?

(ii) can we find an optimal prediction level or magnitude, and optimal durations for the parameter and prediction windows?

(iii) do the results lend themselves to the identification of areas of strengths and weaknesses and hence to future developments of better models?

Let us now discuss some constraints in our choice of window lengths.

1) Prediction window

- Since the prediction window relies on an extrapolation of the parameter window, we feel that the prediction window must not be of a greater duration than the parameter window.

- If the prediction window is too short, the hazard hovers around zero and if it is too long it hovers around 1.

2) Parameter window

- The parameter window cannot be too short, for then there will be an insufficient number of events to perform meaningful statistics.

- Too long a window, on the other hand, will result in an excessive smoothing effect, so that the hazard function will not be sensitive to local trends.

Inspection of Fig. (3.3) on led naturally to the visual identification of three clusters on the VCR as depicted in Fig. (3.6). The coordinates of the apices of the clusters are as follows:

Cluster 1 {(29558, -41761), (29352, -41420), (29051, -41384), (29119, -41846), (29232, -41936)}

Cluster 2 {(29233, -42343), (28880, -41894), (28171, -41894), (28086, -42001), (29092, -42476)}

Cluster 3 {(28752, -42923), (28680, -42457), (28486, -42325), (28054, -42251), (27834, -42300), (28005, -43110), (28054, -43137)}

The clusters are then prisms, truncated top and bottom according to the scheme described in Chapter 2.

Applying Program (E.3) to the entire catalog of events enables us to obtain all the information we require about each of these clusters. A summary of this information is given in the three Tables below.

Note: All quantities are measured in S.I. units unless otherwise stated.

Table 3.1 Particulars regarding cluster 1 on the VCR

Cluster clust_1.vcr contains	2002 events
An average of 3.40 events per day over 1.6 years	
Total Cluster Moment	= 2.082912e+14
Total Cluster Energy	= 2.872218e+09
Maximum Moment	= 7.360000e+12
Minimum Moment	= 2.750000e+08
Maximum Energy	= 2.920000e+08
Minimum Energy	= 2.060000e+02
Average Moment	= 1.040416e+11
Average Energy	= 1.434674e+06
Gamma	= 7.251930e+04

Table 3.2 Particulars regarding cluster 2 on the VCR

Cluster clust_2.vcr contains	3275 events
An average of 5.57 events per day over 1.6 years	
Total Cluster Moment	= 3.346618e+14
Total Cluster Energy	= 1.085200e+10
Maximum Moment	= 1.910000e+13
Minimum Moment	= 1.820000e+08
Maximum Energy	= 2.620000e+09
Minimum Energy	= 1.020000e+02
Average Moment	= 1.021868e+11
Average Energy	= 3.313589e+06
Gamma	= 3.083872e+04

Table 3.3 Particulars regarding cluster 3 on the VCR

Cluster clust_3.vcr contains	4468 events
An average of 7.60 events per day over 1.6 years	
Total Cluster Moment	= 7.528824e+14
Total Cluster Energy	= 4.115475e+10
Maximum Moment	= 1.000000e+14
Minimum Moment	= 1.450000e+08
Maximum Energy	= 1.930000e+10
Minimum Energy	= 5.340000e+01
Average Moment	= 1.685055e+11
Average Energy	= 9.211001e+06
Gamma	= 1.829394e+04

The first bit of information that we are interested in is the value of γ, and this should be characteristic of the clusters as a whole. The reason we insist on this is that it is conceivable that a single event in a cluster can radiate more energy than all the other events in the cluster put together, and this will distort γ terribly and is not what we're after. Also, the cascade of events prematurely triggered by blasting cannot be said to be "typical". Inspection of the three tables above shows a great diversity in the value of γ and suggests that the mechanisms described are playing a significant rôle here.

To overcome this problem, we turn our attention to Fig. (3.7) and notice that if we cut out all events between the times of 15:00 and 20:00 we will cut out the majority of prematurely triggered events and if we restrict the maximum event moment and maximum event energy to values , say, of 1e12 Nm and 1e8 J respectively, we have a good chance of obtaining a characteristic γ. The test for this of course, will be if the calculated value of γ for all 3 clusters happen to be identical.

After implementing the restrictions in the above paragraph, the following results were obtained.

Table 3.4 Particulars of cluster 1 (VCR) after restrictions

Cluster clust_1.vcr (cut) contains 1001 events	
An average of 1.70 events per day over 1.6 years	
Total Cluster Moment	= 4.576632e+13
Total Cluster Energy	= 4.333911e+08
Maximum Moment	= 9.720000e+11
Minimum Moment	= 2.750000e+08
Maximum Energy	= 3.080000e+07
Minimum Energy	= 2.060000e+02
Average Moment	= 4.572060e+10
Average Energy	= 4.329582e+05
Gamma	= 1.056005e+05

Table 3.5 Particulars of cluster 2 (VCR) after restrictions

Cluster clust_2.vcr (cut) contains 1559 events	
An average of 2.65 events per day over 1.6 years	
Total Cluster Moment	= 5.183768e+13
Total Cluster Energy	= 4.411739e+08
Maximum Moment	= 1.000000e+12
Minimum Moment	= 1.820000e+08
Maximum Energy	= 2.700000e+07
Minimum Energy	= 1.020000e+02
Average Moment	= 3.325060e+10
Average Energy	= 2.829852e+05
Gamma	= 1.174994e+05

Table 3.6 Particulars of cluster 3 (VCR) after restrictions

Cluster clust_3.vcr (cut) contains 1844 events	
An average of 3.14 events per day over 1.6 years	
Total Cluster Moment	= 7.319084e+13
Total Cluster Energy	= 7.847045e+08
Maximum Moment	= 9.800000e+11
Minimum Moment	= 1.450000e+08
Maximum Energy	= 4.630000e+07
Minimum Energy	= 5.340000e+01
Average Moment	= 3.969134e+10
Average Energy	= 4.255448e+05
Gamma	= 9.327184e+04

As one can see immediately, we have for all intents and purposes achieved our aim and can safely take γ to be 1.05e5 and use this value as being generally representative of events in the area occupied by the three clusters on the VCR.

We are now in a position to calculate what we term magnitude for *all* the events in the clusters, according to the formula $x = \log(M_0 + \gamma E)$ which has already been mentioned in previous chapters.

We now invoke Program (E.5) - which acts on the entire data set of each cluster in turn - and use its output to plot three log(cumulative frequency) vs. magnitude curves. From these graphs, the cutoff magnitude x_0 (threshold of completeness) is determined. The results of this exercise were as follows:

Cluster 1 $x_0 = 10.375$

Cluster 2 $x_0 = 10.125$

Cluster 3 $x_0 = 10.125$

We are now finally in a position to calculate the hazard for each of the clusters throughout the 588 days that span the catalog. To check the accuracy of our prediction, we use Program (E.6) to list all the actual events which occurred in the cluster having magnitude equal to or greater than some specified value, which in this case will be taken to be the prediction magnitude x_M. (There is a good case for taking this magnitude somewhat lower than x_M but we won't do so here).

A useful constraint on x_M is obtained from the fact that we want between 10 and 40 events say, with magnitude $\geq x_M$ in each of the clusters under consideration - more than this just clutters up the picture.

Let us now turn our attention to Program (E.7). The first thing to notice is that the user inputs three major parameters viz. the Prediction window duration, the Prediction magnitude, and the Parameter window duration. Numerous combinations of these three parameters were tried on all three clusters, and the results were all much the same when compared to the actual occurrence of events equal to or above the prediction magnitude. Therefore, only a typical set of results is displayed in Fig. (3.8) and a zoomed in section, between days 300 and 470 for all four charts, is given in Fig. (3.9).

The parameter details are as follows.

Cluster 1 (VCR)

Prediction magnitude held fixed at 12.75.

Chart (A)	Parameter window = 20 days	and prediction window	= 14 days.
Chart (B)	Parameter window = 45 days	and prediction window	= 28 days.
Chart (C)	Parameter window = 75 days	and prediction window	= 54 days.
Chart (D)	Parameter window = 100 days	and prediction window	= 72 days.

The actual events in the cluster having magnitude ≥ 12.75 are superposed on the hazard charts as short vertical lines resembling bar codes .

A convex cluster having apices {(29208, -42642), (26987, -42642), (26169, -43859), (26987, -45011), (28701, -45011)} was tried on the CLR, following essentially the same procedure as with the clusters on the VCR, but again, the results yielded nothing new.

It was now decided to treat the entire VCR as a single cluster and also the entire CLR as a single cluster. Again, the same procedure as before was followed. The overall statistics, before and after cutting out the blasting times and the outstandingly large events, are shown for the VCR and CLR respectively.

Table 3.7 Particulars regarding the entire VCR

Cluster allvcr contains	19050 events
An average of 32.40 events per day over 1.6 years	
Total Cluster Moment	= 3.435072e+15
Total Cluster Energy	= 2.095121e+11
Maximum Moment	= 1.380000e+14
Minimum Moment	= 8.170000e+07
Maximum Energy	= 4.350000e+10
Minimum Energy	= 4.080000e+01
Average Moment	= 1.803187e+11
Average Energy	= 1.099801e+07
Gamma	= 1.639558e+04

Table 3.8 Particulars regarding the entire CLR

Cluster allcl contains	18302 events
An average of 31.13 events per day over 1.6 years	
Total Cluster Moment	= 5.722023e+15
Total Cluster Energy	= 1.493800e+12
Maximum Moment	= 4.600000e+14
Minimum Moment	= 9.490000e+07
Maximum Energy	= 3.740000e+11
Minimum Energy	= 3.240000e+01
Average Moment	= 3.126447e+11
Average Energy	= 8.161949e+07
Gamma	= 3.830515e+03

Table 3.9 Particulars of the entire VCR after restrictions

Cluster allvcr (cut) contains	8966 events
An average of 15.25 events per day over 1.6 years	
Total Cluster Moment	= 3.906795e+14
Total Cluster Energy	= 4.438563e+09
Maximum Moment	= 1.000000e+12
Minimum Moment	= 8.170000e+07
Maximum Energy	= 9.210000e+07
Minimum Energy	= 4.080000e+01
Average Moment	= 4.357345e+10
Average Energy	= 4.950438e+05
Gamma	= 8.801937e+04

Table 3.10 Particulars of the entire CLR after restrictions

Cluster allcl (cut) contains	11084 events
An average of 18.85 events per day over 1.6 years	
Total Cluster Moment	= 3.744291e+14
Total Cluster Energy	= 1.294565e+10
Maximum Moment	= 9.930000e+11
Minimum Moment	= 9.860000e+07
Maximum Energy	= 9.950000e+07
Minimum Energy	= 3.240000e+01
Average Moment	= 3.378104e+10
Average Energy	= 1.167958e+06
Gamma	= 2.892316e+04

The outcome, is that for the entire reefs, we find that:

$\gamma_{(VCR)} = 88020$

$\gamma_{(CLR)} = 3923$

Using these values of γ we are able to draw the log(cumulative frequency) vs. magnitude graphs for the VCR and the CLR and they are displayed jointly in Fig. (3.10).

In the case of the VCR the cutoff magnitude x_0 was deemed to be 10.125 and in the case of the CLR, 9.125 .

After many attempts at trying to find optimal window durations and prediction magnitudes, to obtain the best match between seismic hazard and the occurrence of actual events, the following was accepted.

For the VCR:

Prediction Magnitude x_M = 14.00

Prediction Window = 32 days

Parameter Window = 45 days

For the CLR:

Prediction Magnitude x_M = 14.75

Prediction Window = 28 days

Parameter Window = 30 days

The occurrence of events with magnitude $\geq x_M$ are shown as magnitude - time bar charts in Fig. (3.11) for both the VCR and the CLR.

Fig. (3.12) displays the hazard for both reefs, and the actual events with magnitudes equal to or above the prediction level are superposed on these graphs as downward pointing arrows. This has been done to expedite the comparison of the probability of occurrence with the actual events.

The results were somewhat more encouraging than for the small clusters so that the logical next step forward was to consider the *entire mine* as a single population of events. To this end we display the before and after statistics as usual, to find the value of γ.

Table 3.11 Particulars regarding the entire mine

Cluster projdata contains	42493 events
An average of 72.27 events per day over 1.6 years	
Total Cluster Moment	= 2.263940e+16
Total Cluster Energy	= 5.080126e+18
Maximum Moment	= 5.980000e+15
Minimum Moment	= 8.170000e+07
Maximum Energy	= 5.080000e+18
Minimum Energy	= 3.240000e+01
Average Moment	= 5.327794e+11
Average Energy	= 1.195521e+14
Gamma	= 4.456464e-03

Table 3.12 Particulars of the entire mine after restrictions

Cluster projdata (cut) contains	22152 events
An average of 37.67 events per day over 1.6 years	
Total Cluster Moment	= 1.131265e+15
Total Cluster Energy	= 3.1[illegible]9393e+10
Maximum Moment	= 1.000000e+12
Minimum Moment	= 8.170000e+07
Maximum Energy	= 9.950000e+07
Minimum Energy	= 3.240000e+01
Average Moment	= 5.106830e+10
Average Energy	= 1.408177e+06
Gamma	= 3.626555e+04

Using $\gamma =$ 36266, we plot the log(cumulative frequency) vs. magnitude or Gutenberg - Richter curve shown in Fig. (3.13). Normally, we would just proceed to find x_0 and then evaluate the hazard. However, inspection of Fig. (3.13) shows that estimating the cutoff point in this case is a little more difficult than in previous cases.

We further make the observation that insisting on a complete set is really too severe a condition, and that actually we are able to get away with a *consistently incomplete* data set in which any variations will, as in the case of the complete set, be attributable to fluctuating physical processes and not to changes in the sensitivity of the monitoring equipment.

Therefore, let us turn our attention to activity rates, viz. the number of events per unit time. Factors which affect the activity rate are:

- changes taking place in the mining conditions, e.g. higher rates of extraction and mining towards unfavourable geological features, etc. i.e. physical conditions, and

- changes in the sensitivity of the monitoring equipment, e.g. higher geophone densities, higher sampling frequencies, more sensitive triggering, etc. i.e. instrumentation.

Let us look at two idealized scenarios; one in which we get a sustained increase in activity rate due entirely to physical conditions, after some time t - see Fig.(3.1) overleaf, and the other, similar in every respect except that the increased activity rate is now due entirely to improved instrumentation, Fig. (3.2) overleaf.

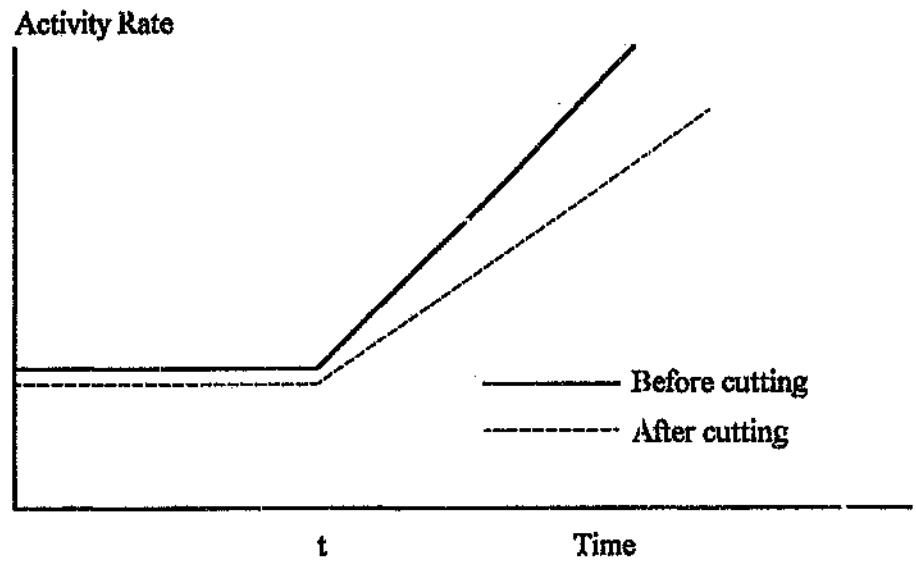


Figure 3.1 Increase in activity rate due to physical reasons

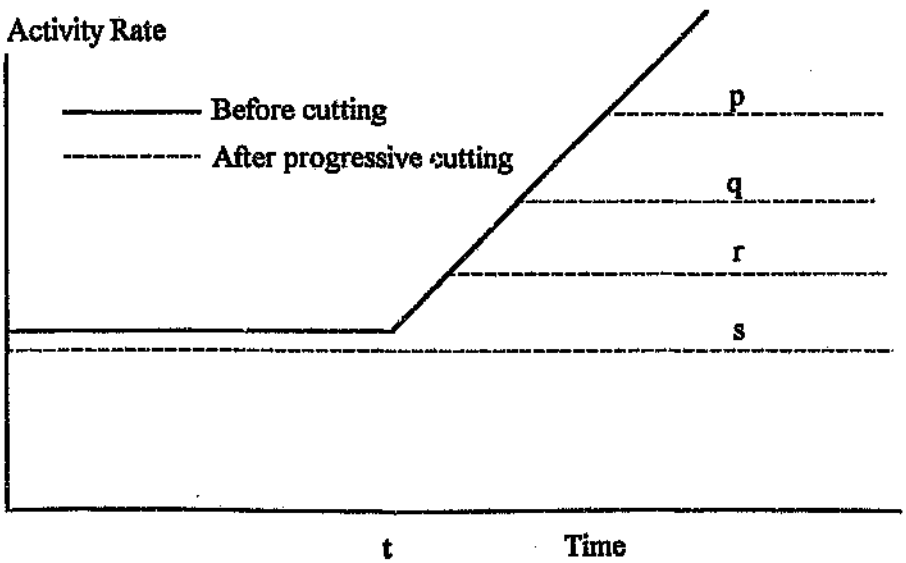


Figure 3.2 Increase in activity rate due to improved instrumentation

(By cutting, we mean excluding from the data set all events having magnitude less than some given value).

We return now to the Gutenberg - Richter diagram and make a tentative cut at x_0 = 10.125. The question now arises: is this enough? And the answer is probably no, if we are after a complete set. But in view of the above deliberations, let us plot the activity rate for the entire mine, before and after cutting at 10.125. The results are shown in Fig. (3.14) and closely resemble the scenario of cut (s) in Fig. (3.2) above. We conclude therefore, that cutting the data set at 10.125, cannot guarantee a complete set, but at least we are certain of having a "system - free" set of data, and that's all that we're really after.

A multitude of various combinations of prediction magnitude, prediction window duration and parameter window durations were tried and only three of the more successful sets have been recorded in this project. They are:

Set 1	Parameter window duration	= 12 days
	Prediction window duration	= 7 days
	Prediction magnitude	= 15.50
Set 2	Parameter window duration	= 30 days
	Prediction window duration	= 20 days
	Prediction magnitude	= 16.00
Set 3	Parameter window duration	= 45 days
	Prediction window duration	= 43 days
	Prediction magnitude	= 16.25

Bar charts of actual events with magnitudes greater than or equal to 15.50, 16.00 and 16.25 are shown in Figures (3.15), (3.16), and (3.17) respectively.

The calculated values of N, β and C for each of the above sets are shown in Figures (3.18) to (3.20) inclusive.

The hazard diagrams for sets 1, 2 and 3 are given in Figures (3.21), (3.22) and (3.23) respectively. As usual, the actual events have been arrowed in so that the success or otherwise of the model can be more easily assessed.

Because Fig.(3.21) is a little crowded, with the probability function (hazard) not being too clearly visible at a first glance, a separate hazard vs. time graph is included - see Fig. (3.24), without the superposition of the "event arrows".

Finally, Fig.(3.25) depicts a linear relationship (Tsubokawa, 1969, 1973) between the moment magnitude and the logarithm of the "precursive time" (parameter window) in days obtained from the 3 sets above. It is noteworthy that this relationship was discovered to hold only after the "input parameters" to evaluate the hazard had been finalized. Our definition of magnitude was converted into moment magnitude in accordance with the formula developed in Appendix A, so that the equation

$$\log(T) = 0.932M_L - 2.4$$

will be more intelligible to those Rock Mechanics Engineers etc. who may want to investigate its potential.

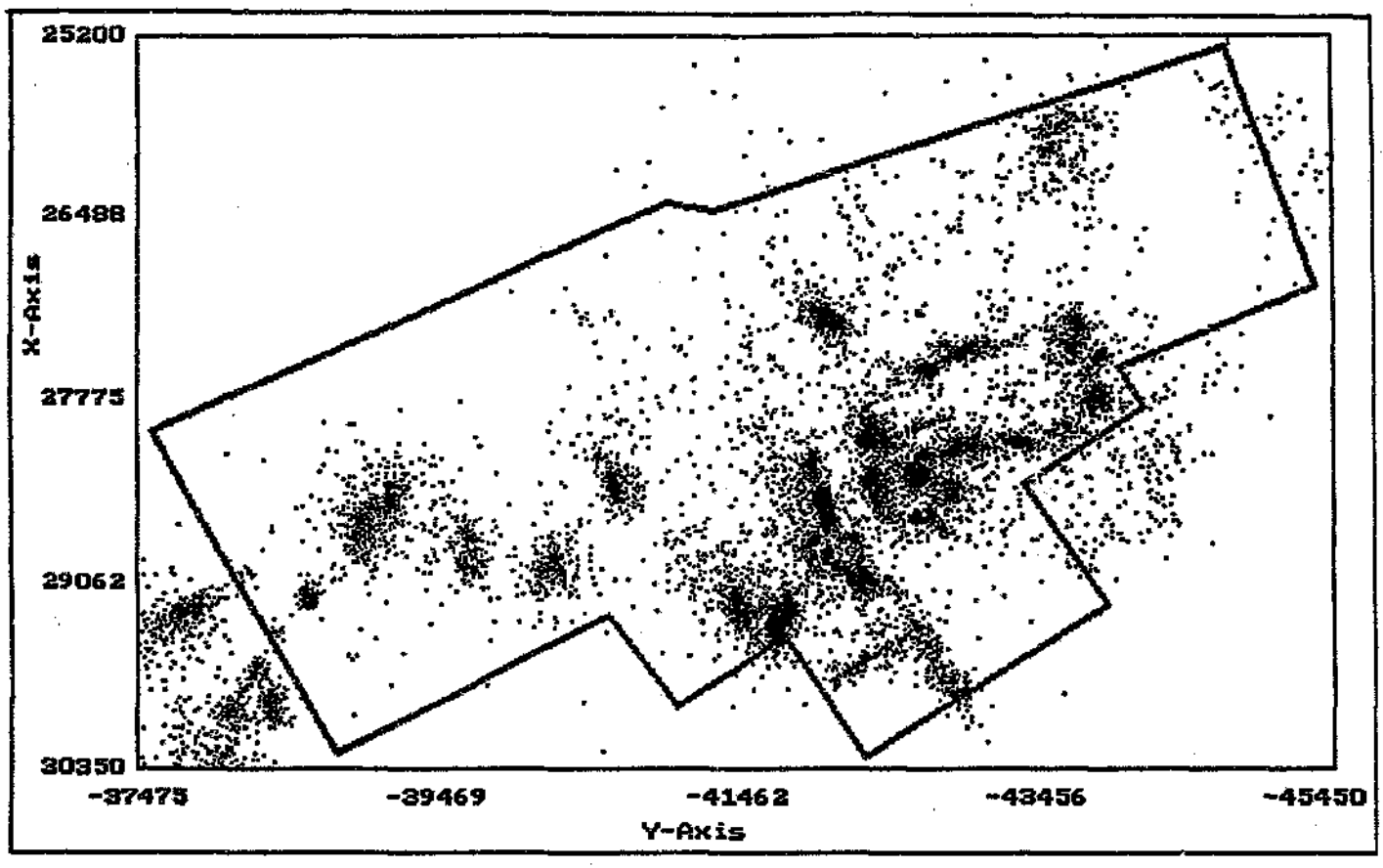


Figure 3.3 Scatter diagram for the VCR events

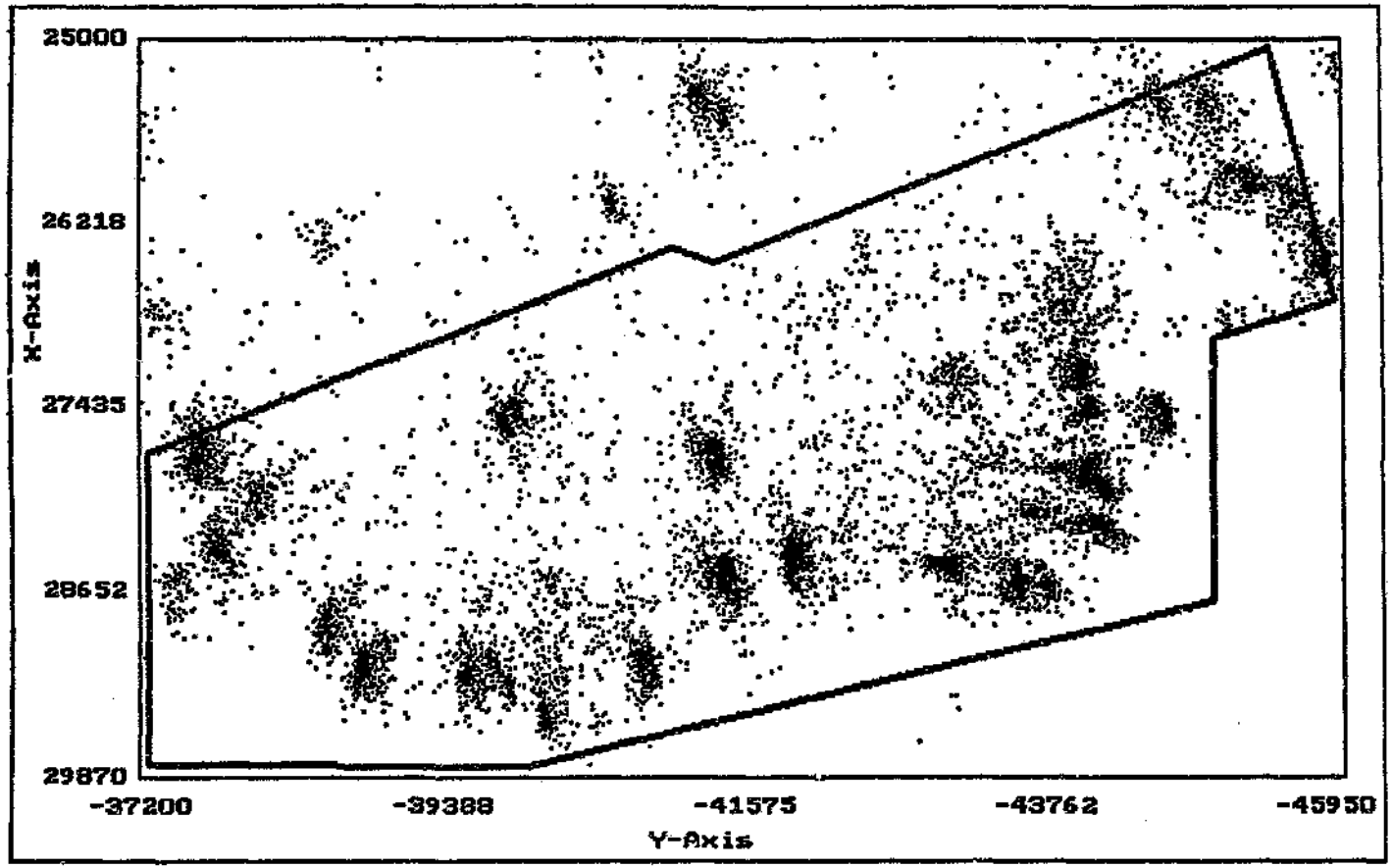


Figure 3.4 Scatter diagram for the CLR events

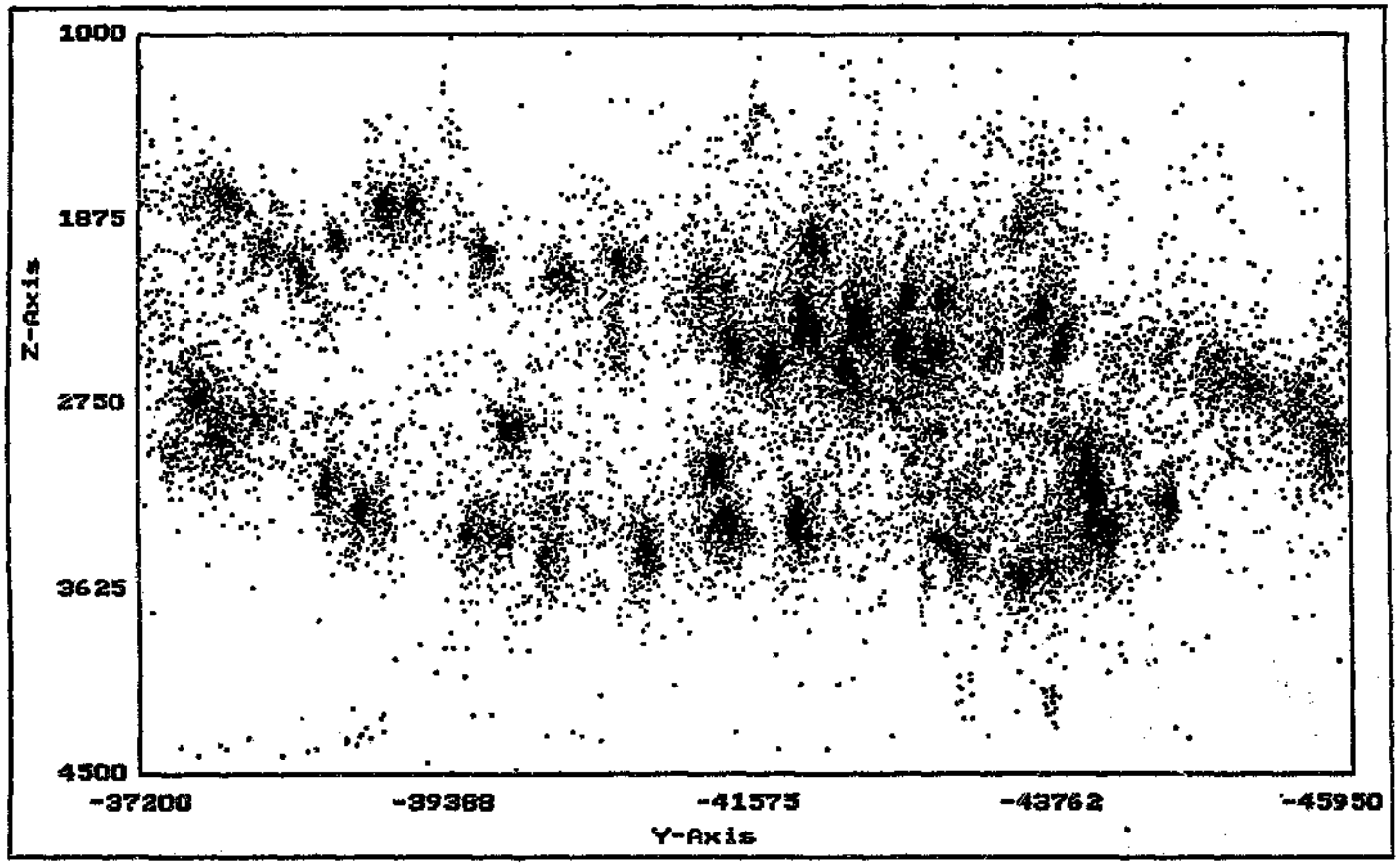


Figure 3.5 Scatter diagram of events in the Y-Z plane

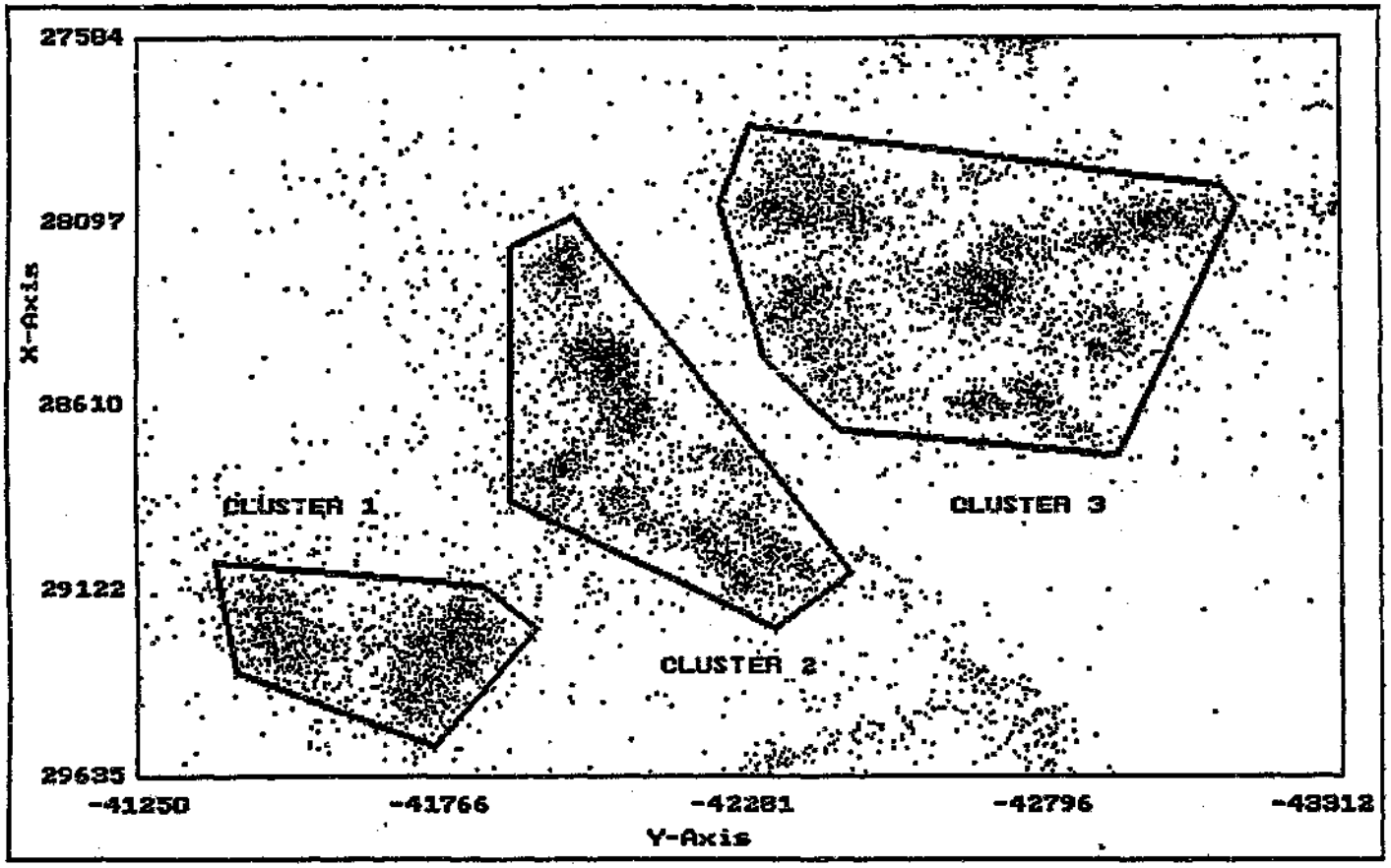


Figure 3.6 Selected clusters on the VCR

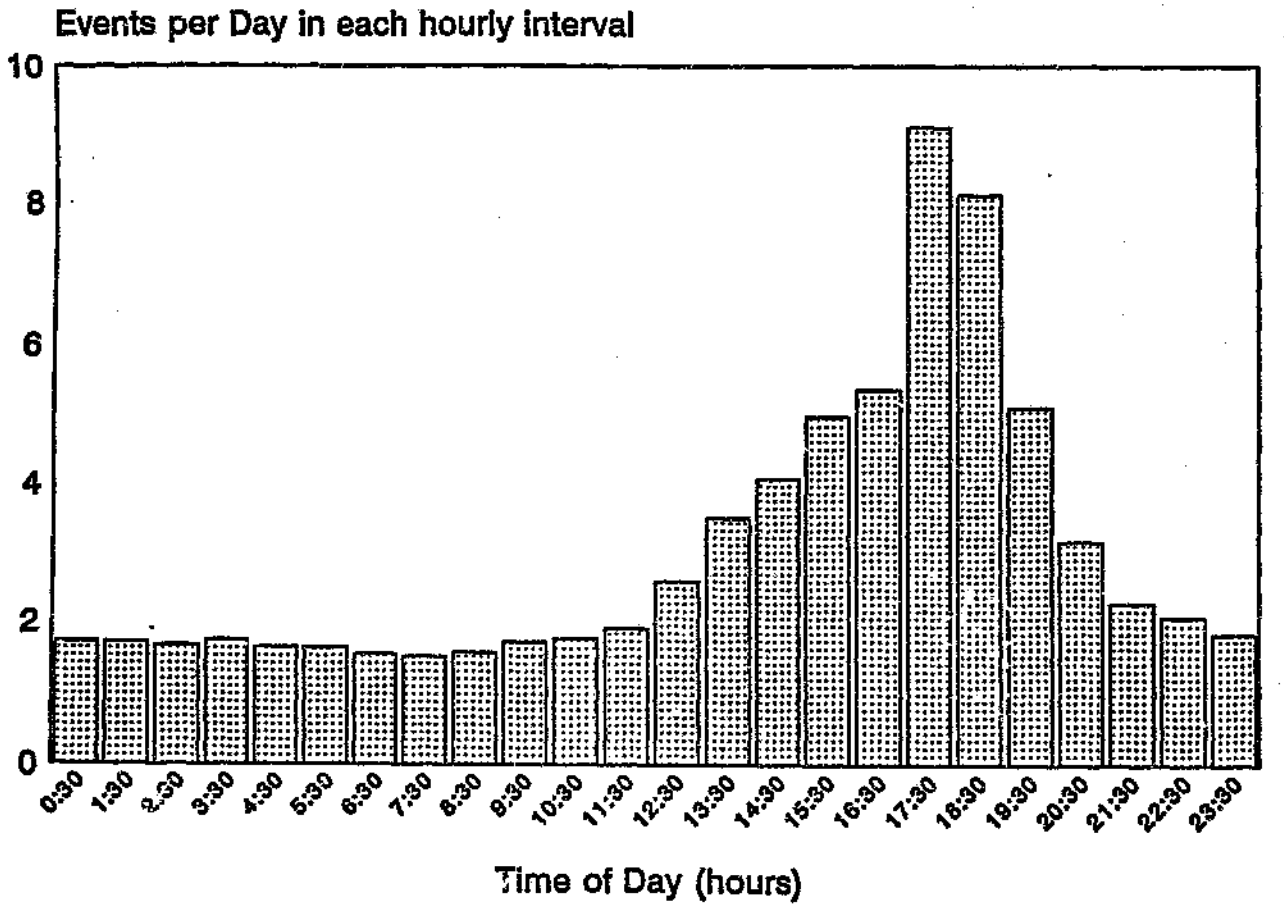


Figure 3.7 The effect of blasting on activity rate

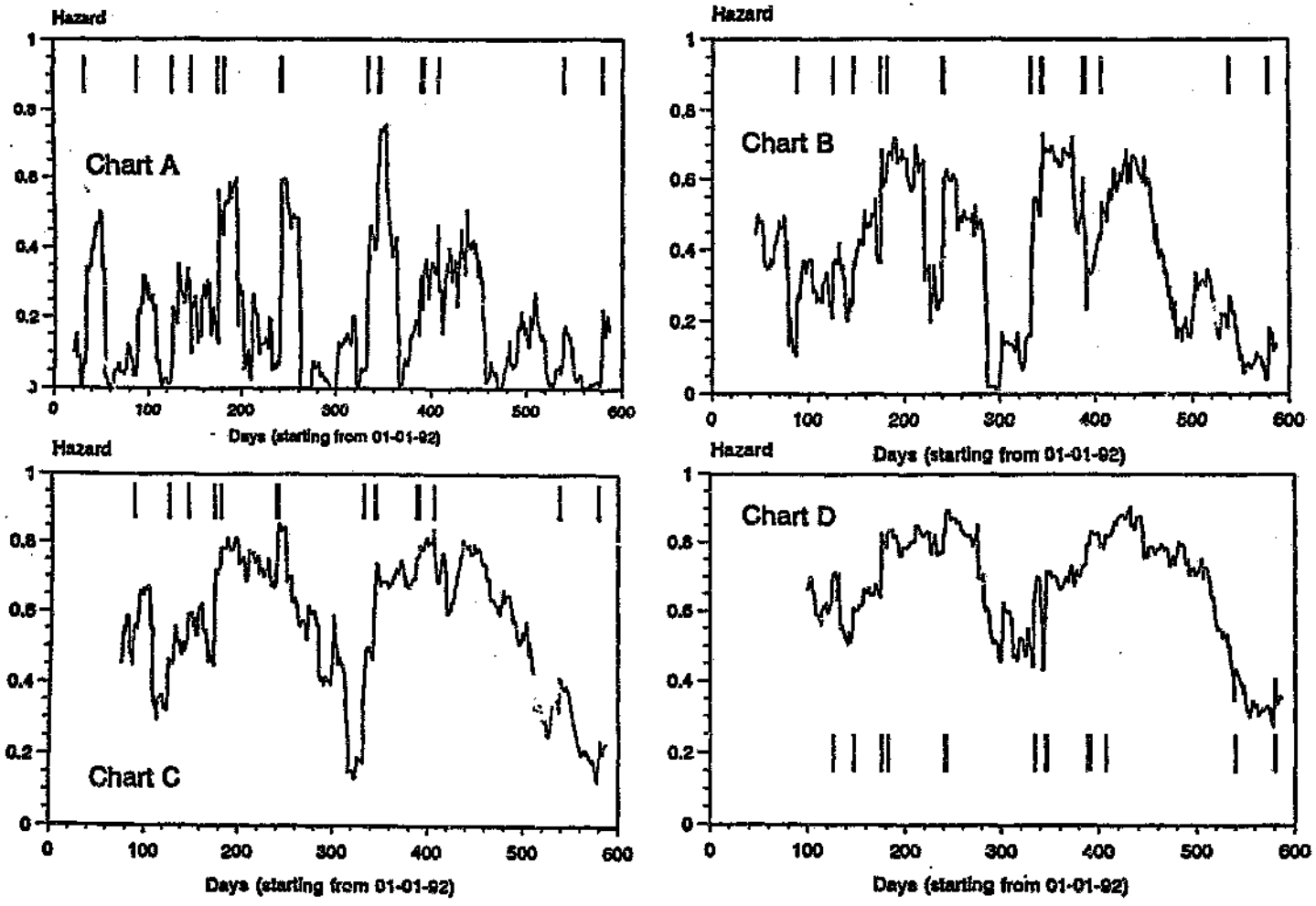


Figure 3.8 Seismic hazard for cluster 1 on the VCR for various parameter windows

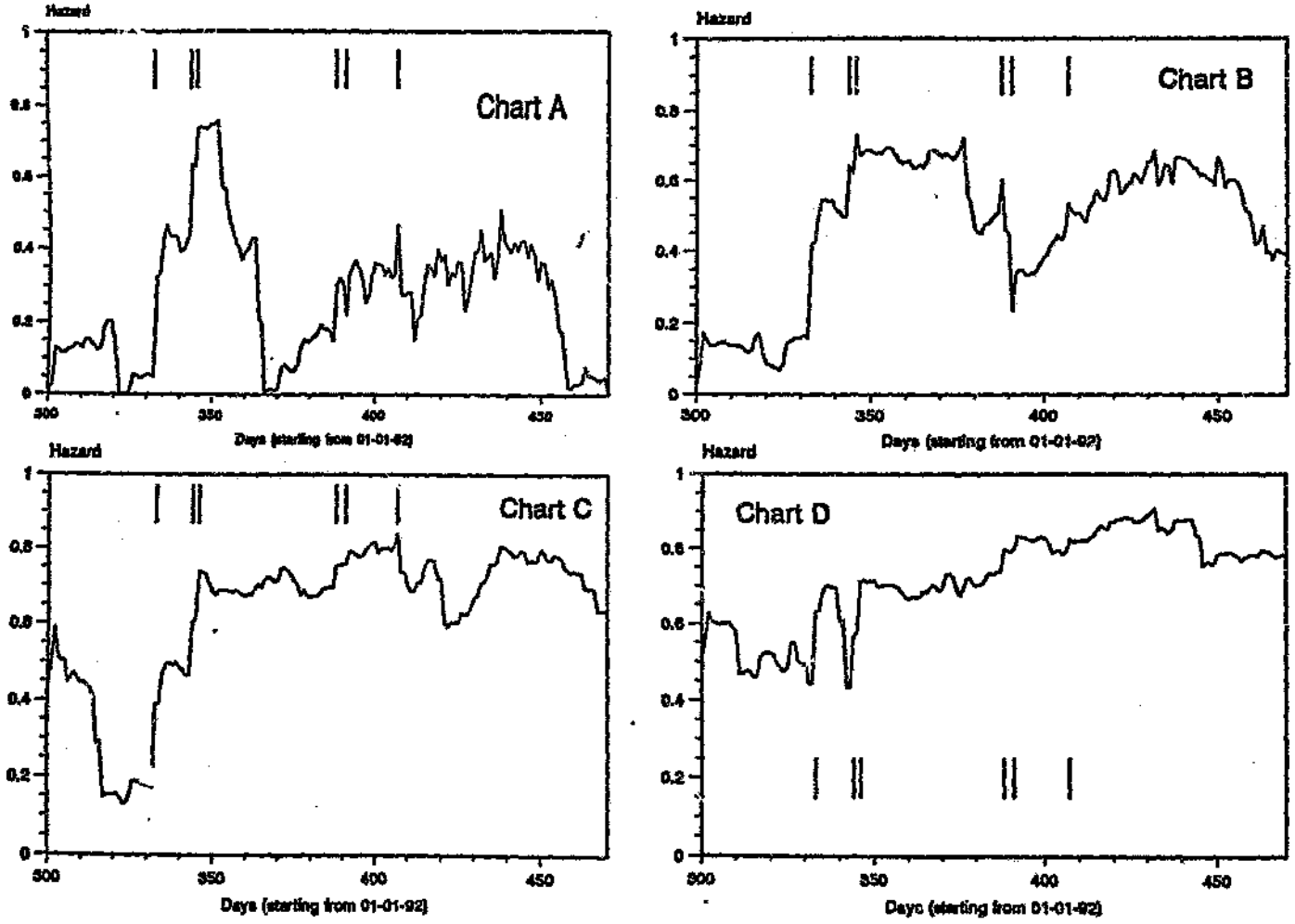
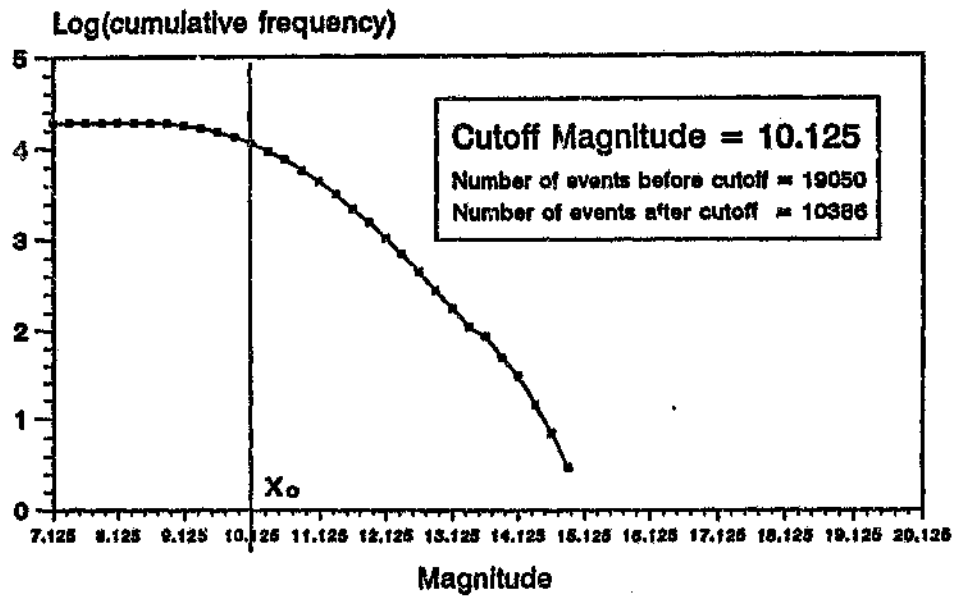


Figure 3.9 Hazard for cluster 1 on the VCR : zoomed in for days 300-470



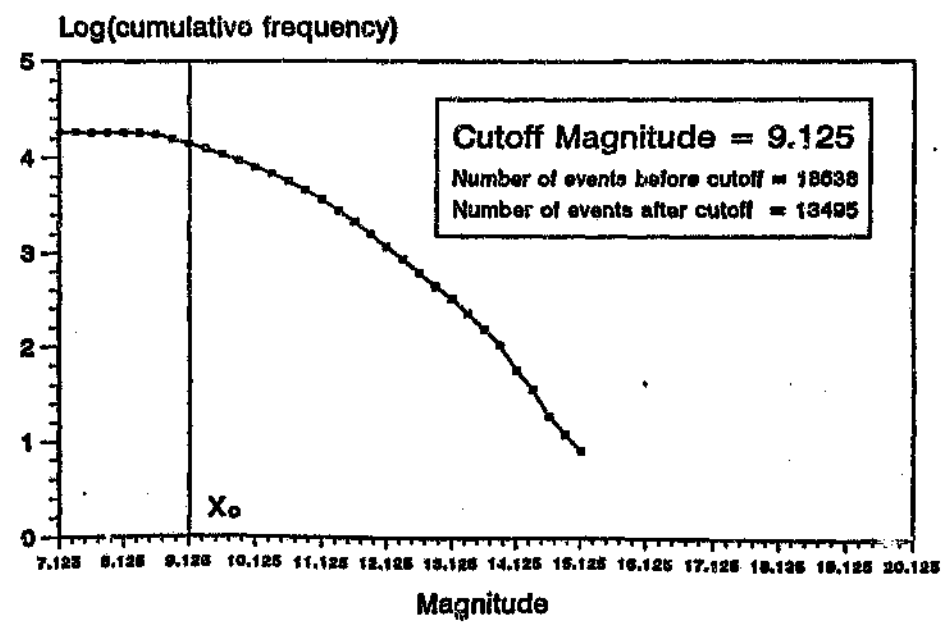


Figure 3.10 Frequency-magnitude relationships for both reefs

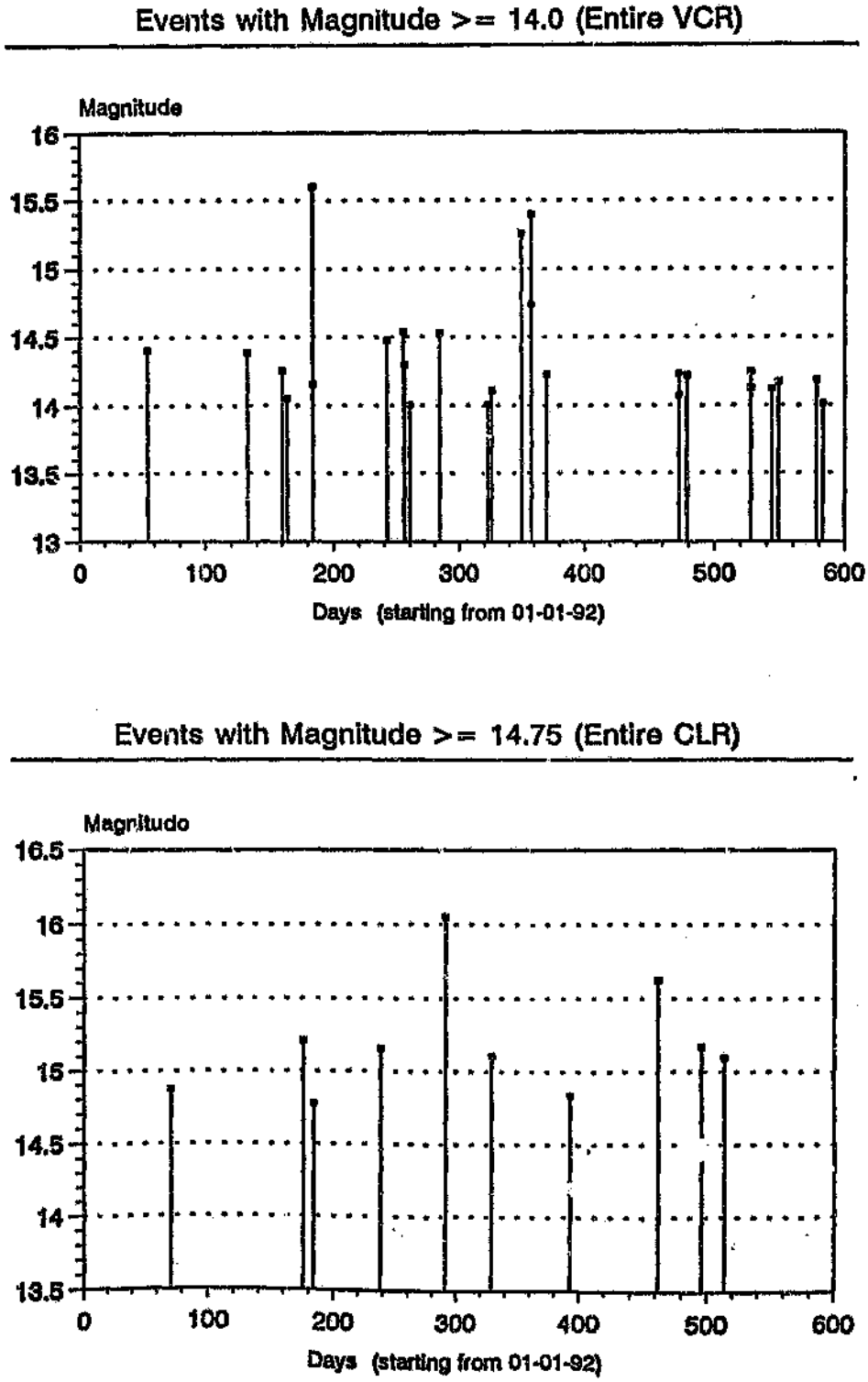
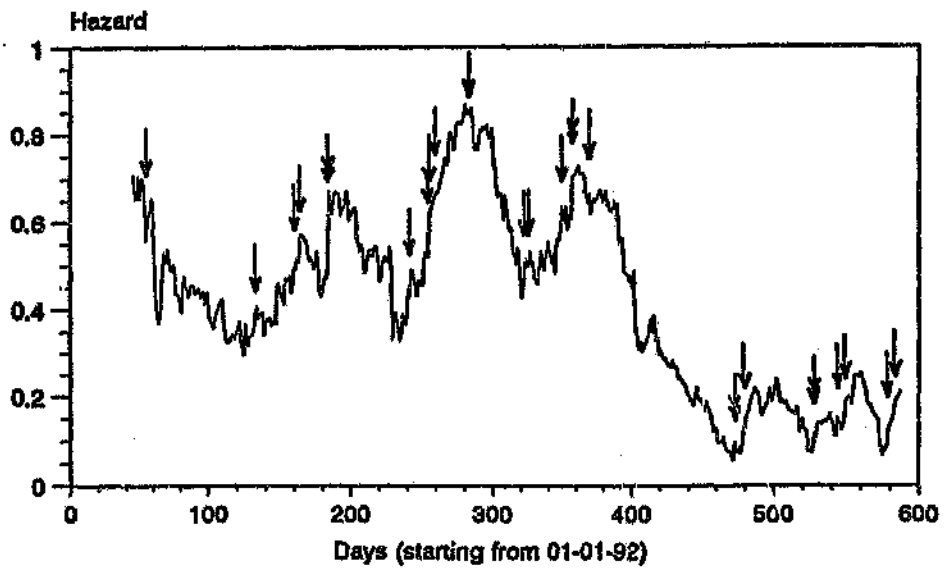


Figure 3.11 Large events on the VCR and CLR



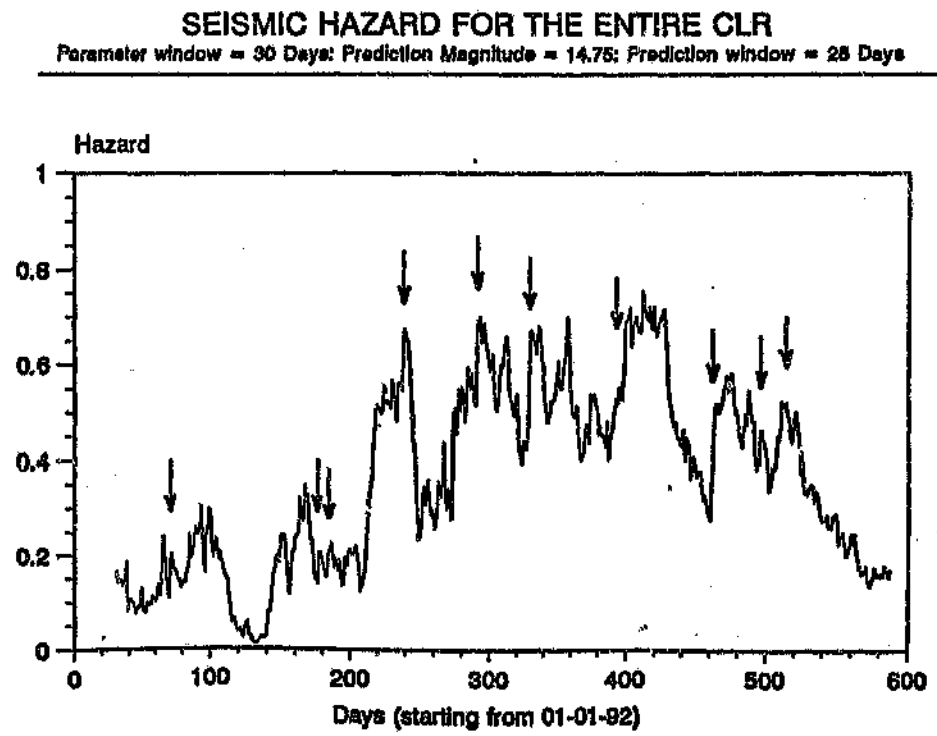


Figure 3.12 Seismic hazard for the VCR and CLR

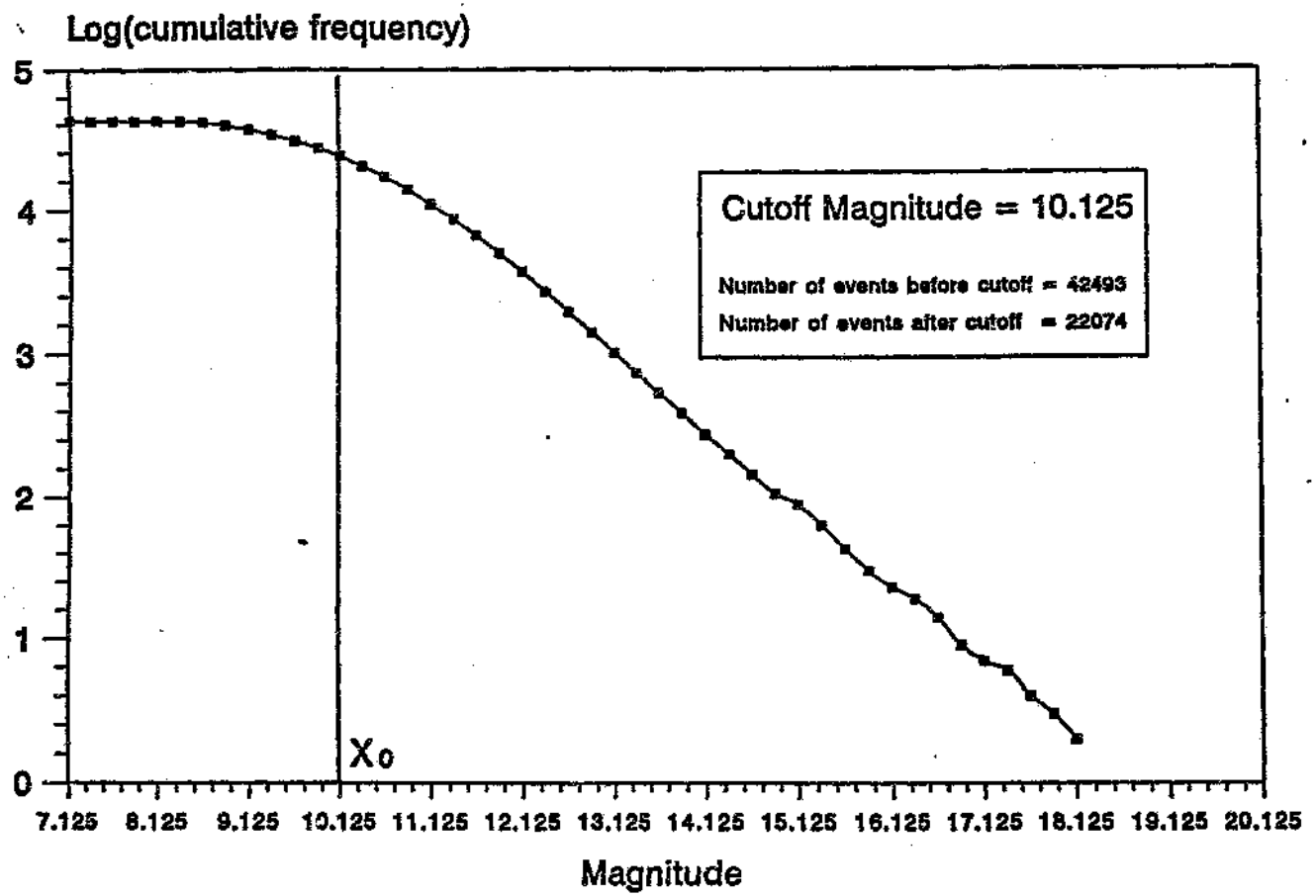


Figure 3.13 Gutenberg-Richter relationship for the entire mine

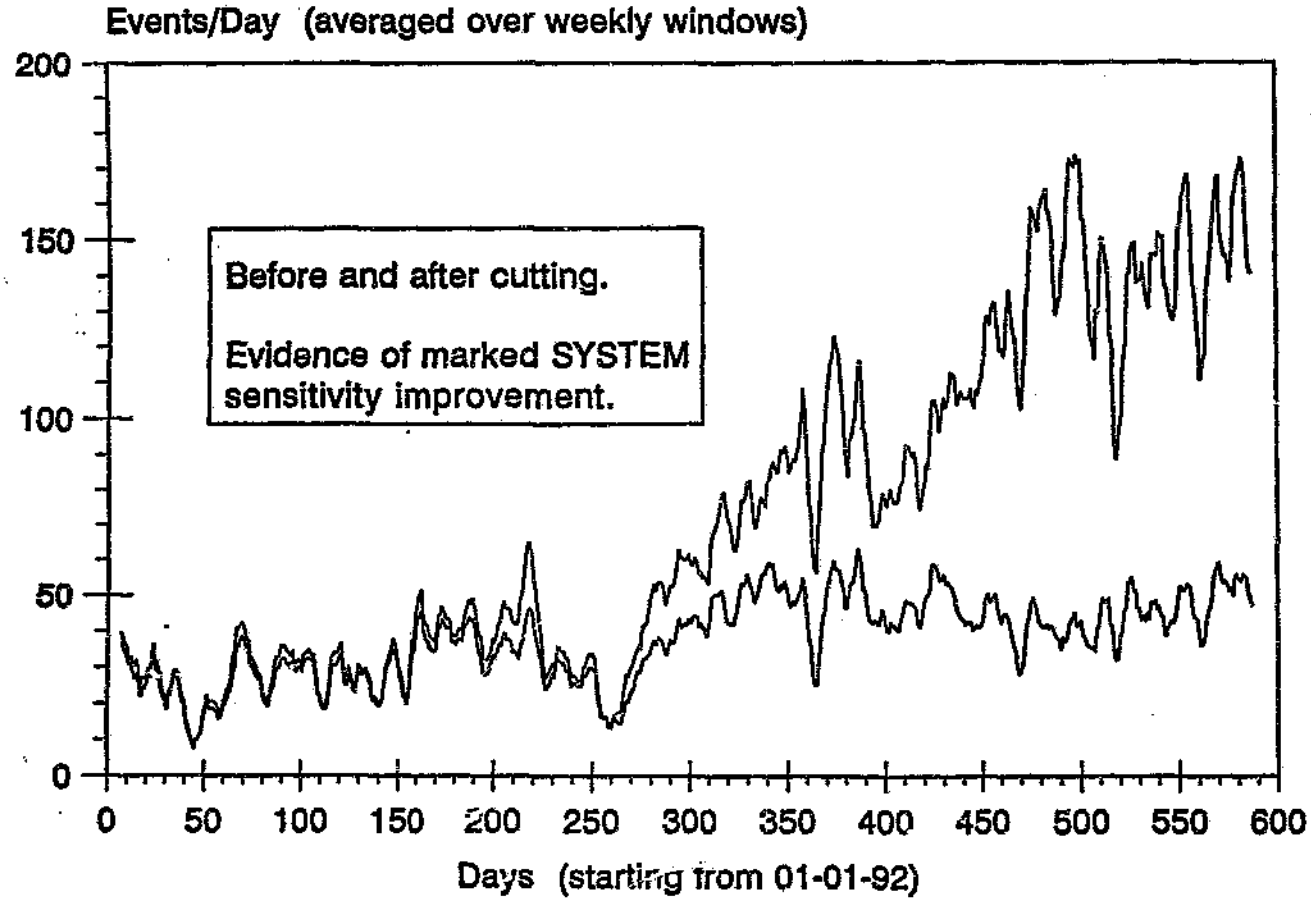


Figure 3.14 Activity rates for the entire mine

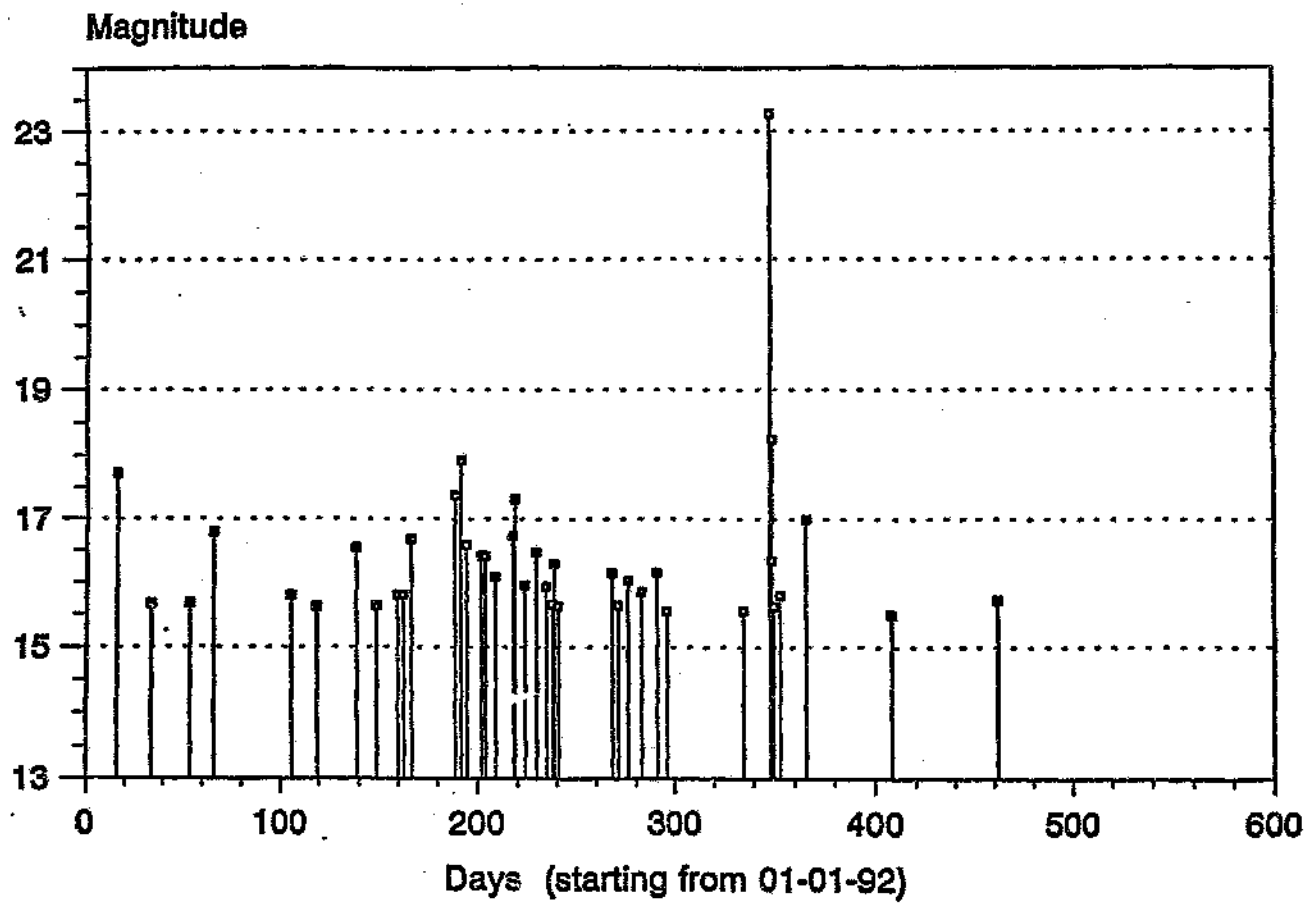


Figure 3.15 Events with magnitude >= 15.50 for the entire mine

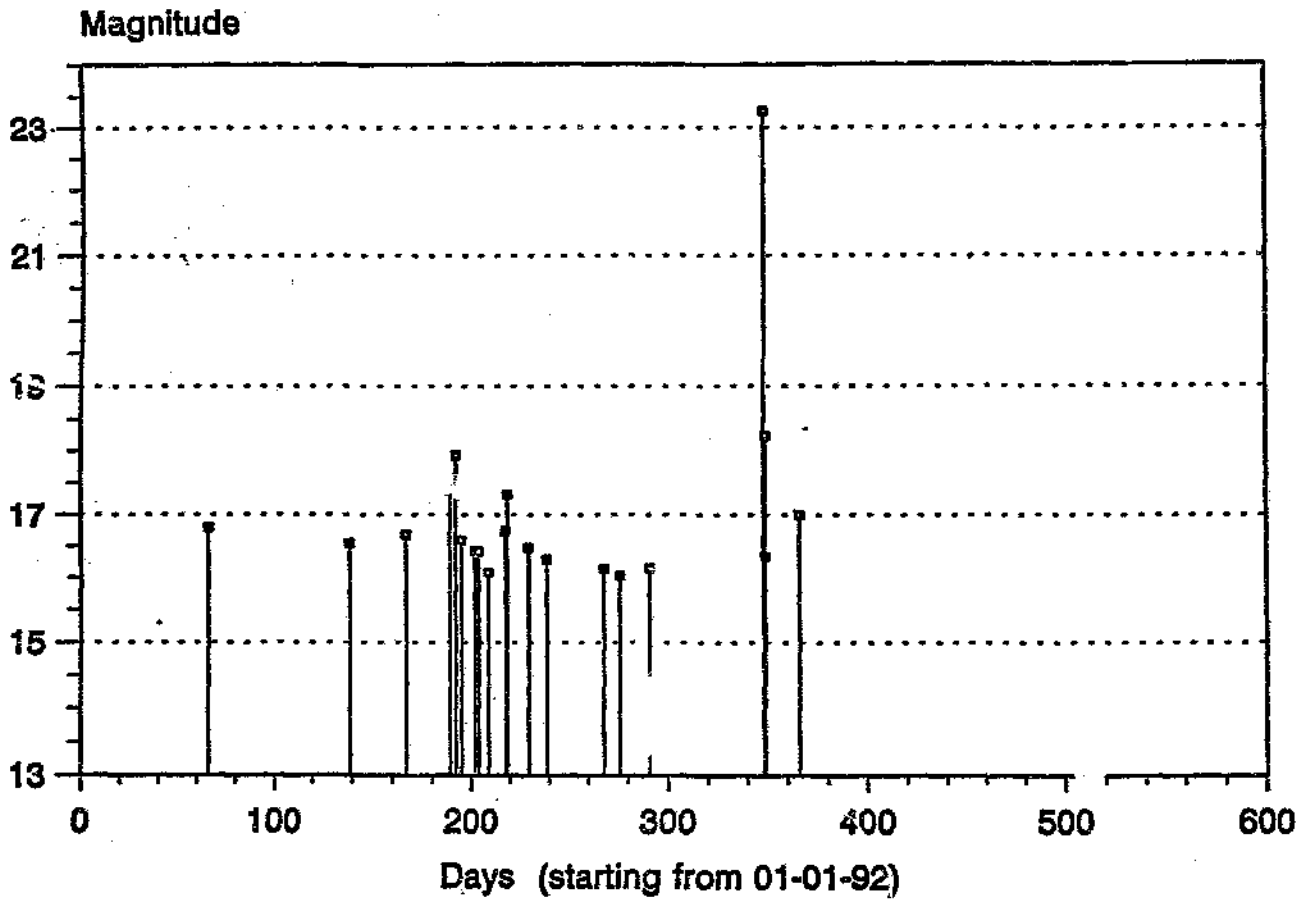


Figure 3.16 Events with magnitude >= 16.00 for the entire mine

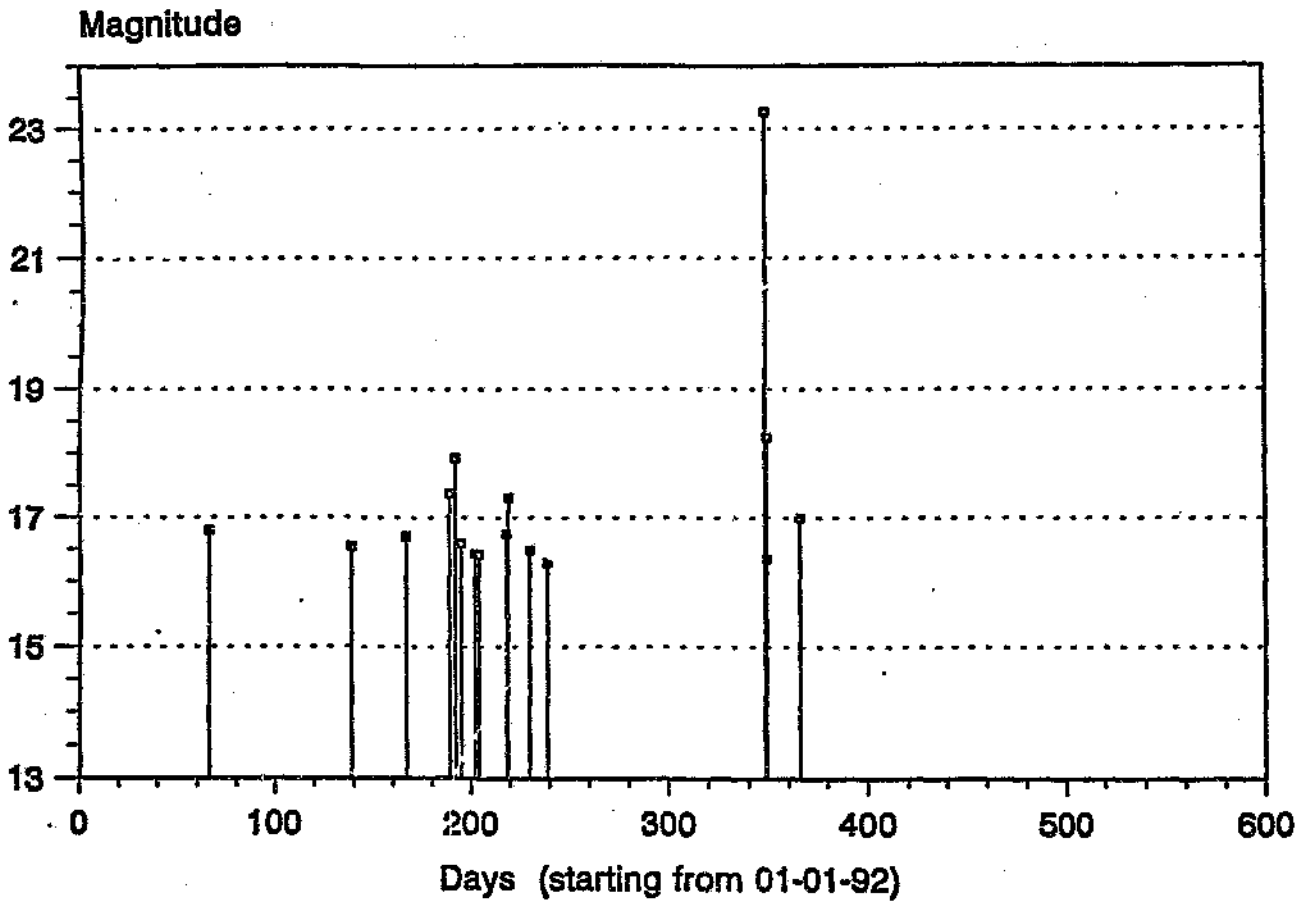
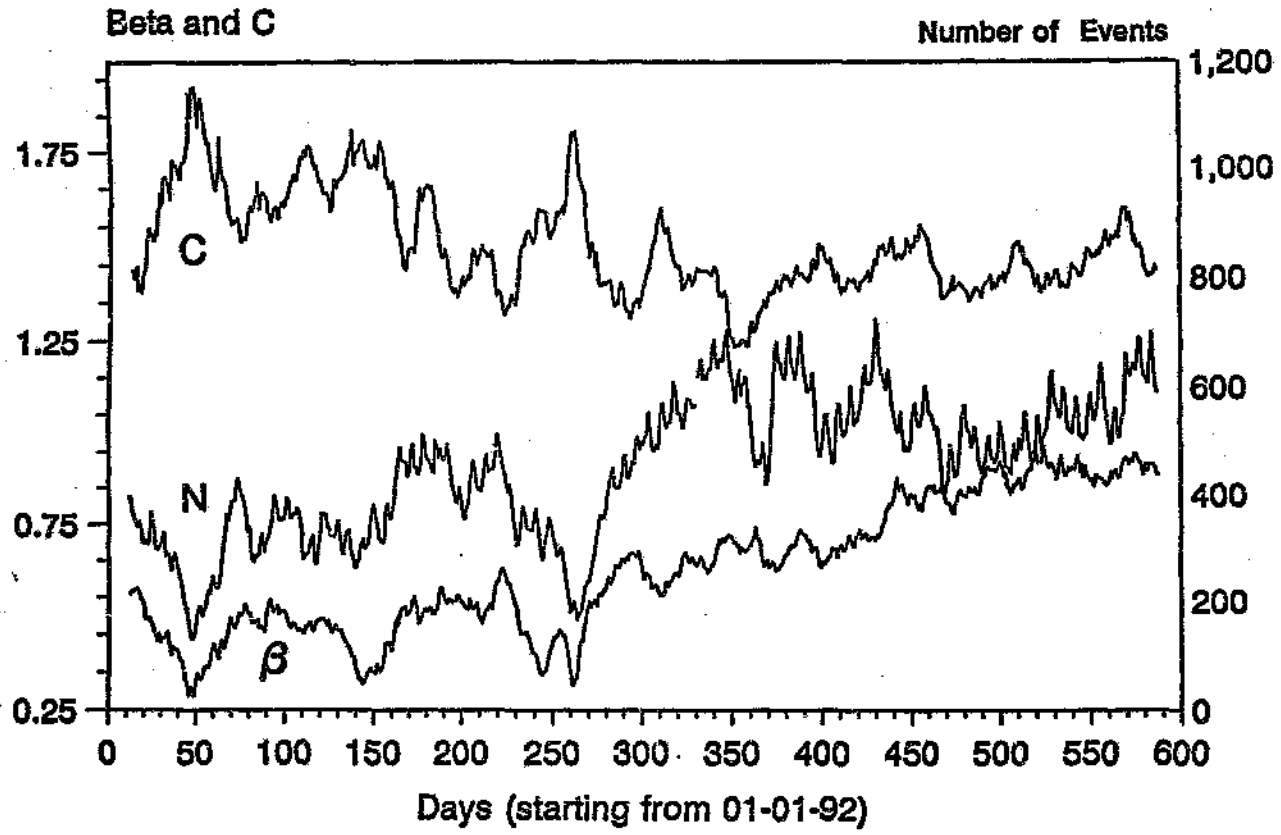
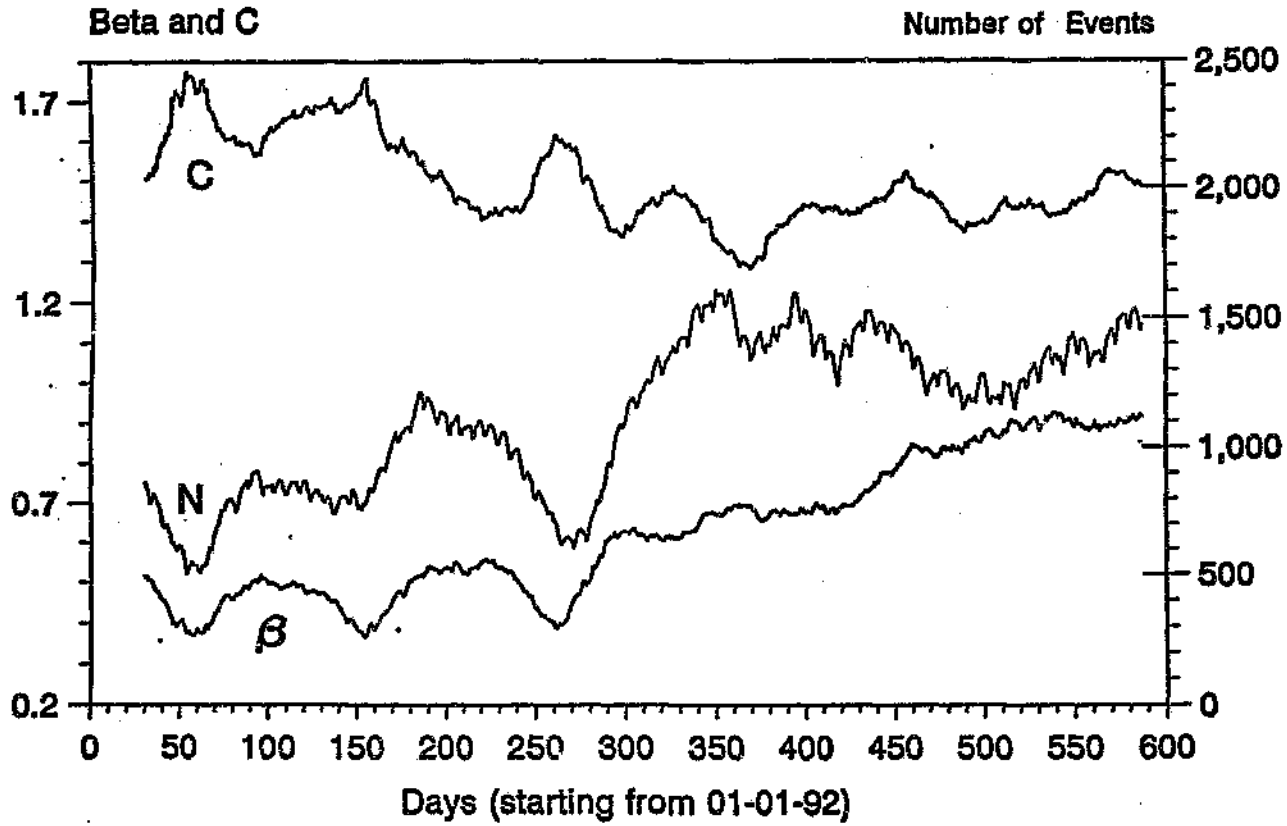


Figure 3.17 Events with magnitude >= 16.25 for the entire mine



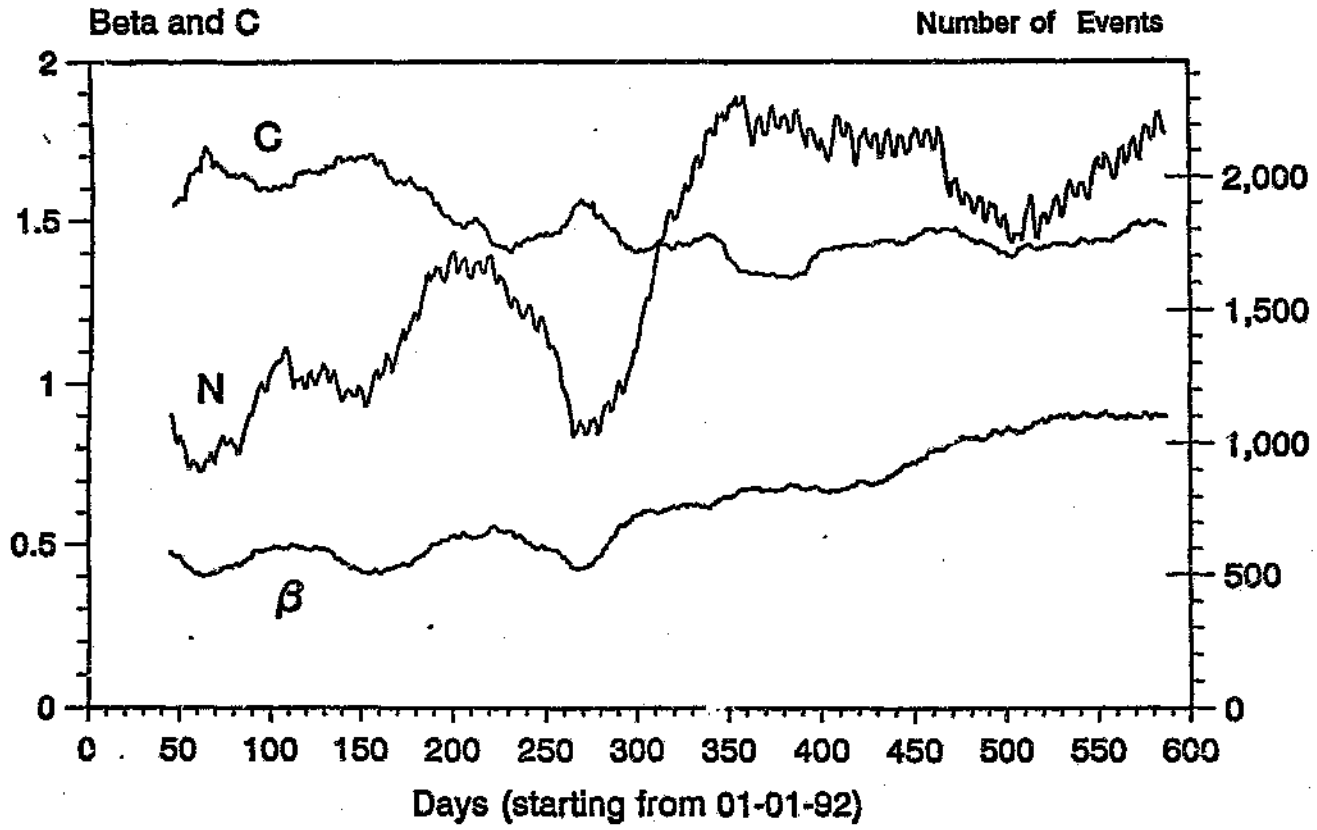
[Parameter window = 12 days; prediction magnitude = 15.50; prediction window = 7 days]

Figure 3.18 Values of beta, C and N in each parameter window (entire mine)



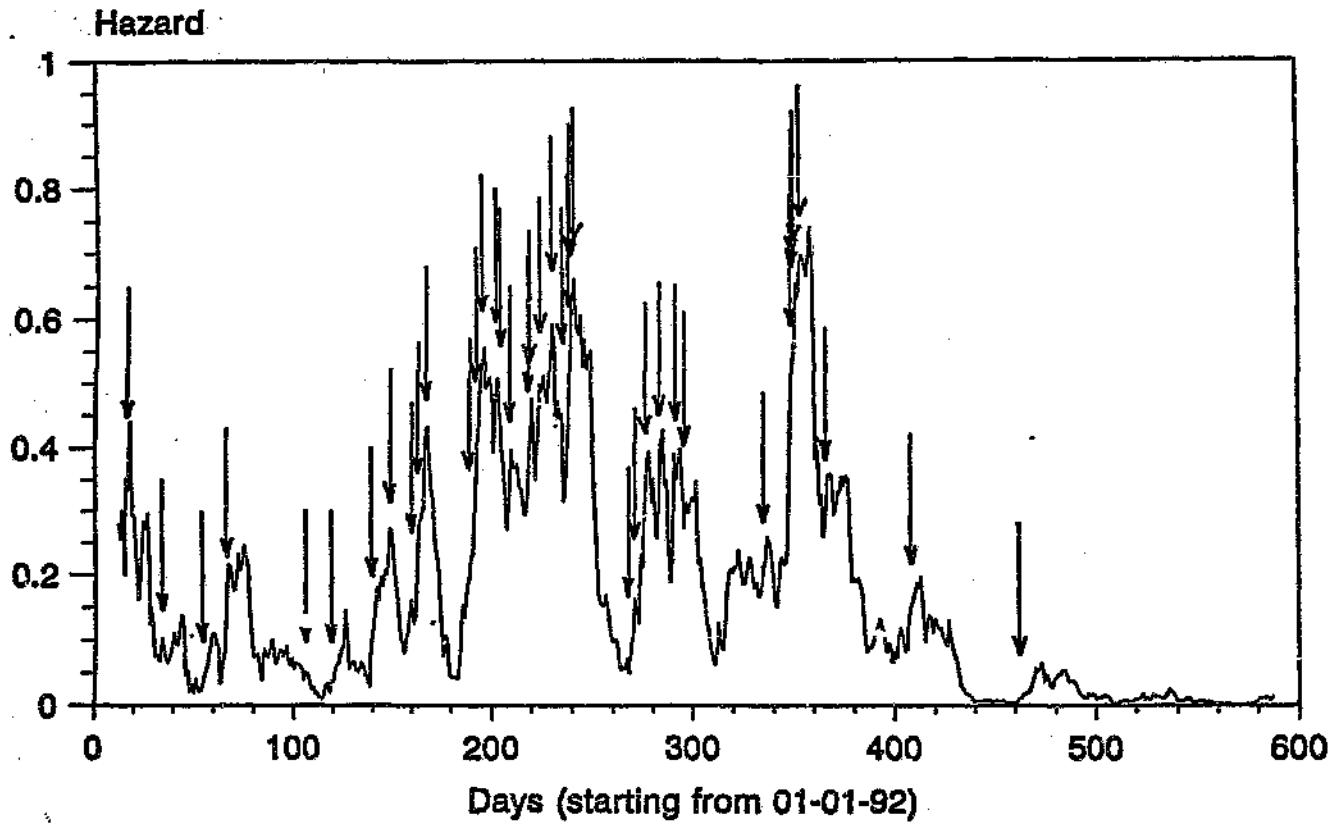
[Parameter window = 30 days; prediction magnitude = 16.00; prediction window = 20 days]

Figure 3.19 · Values of beta, C and N in each parameter window (entire mine)



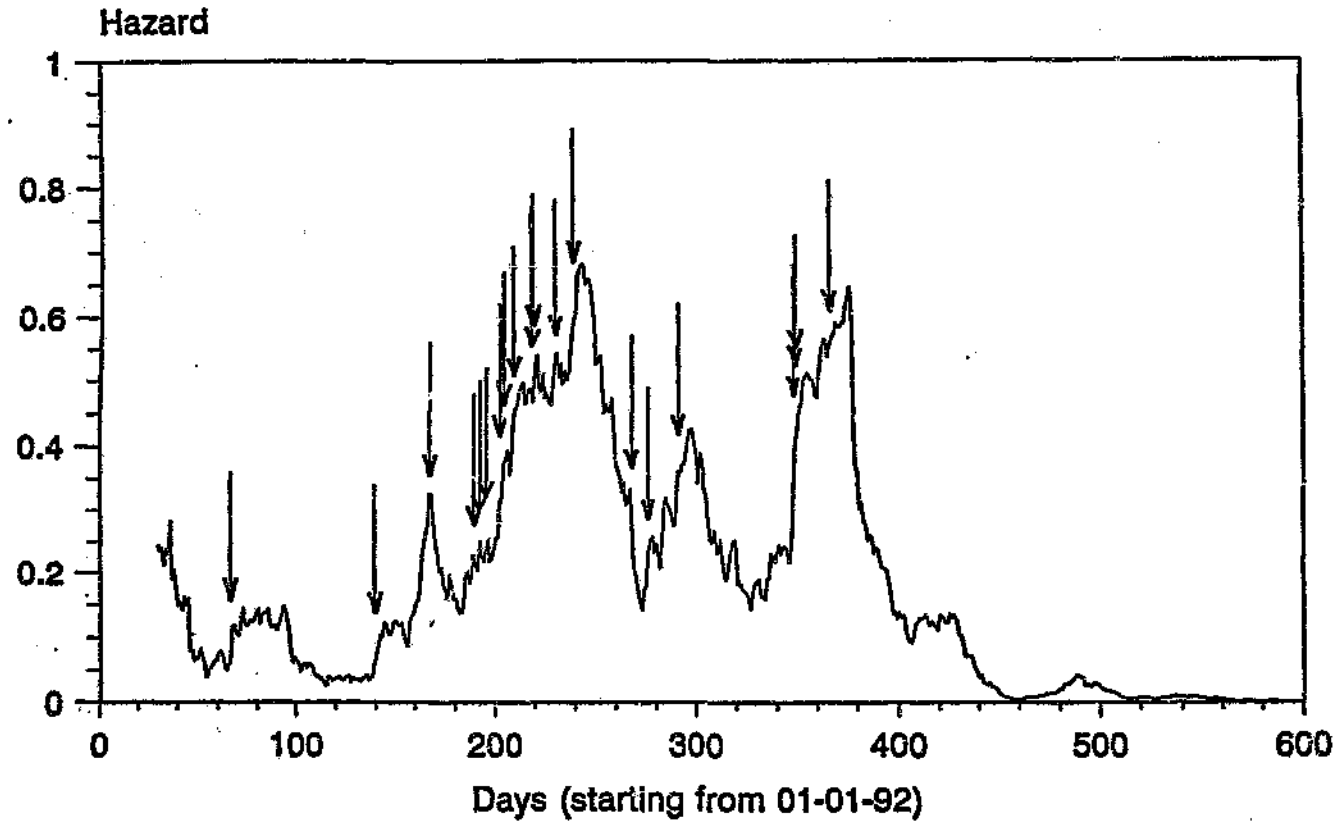
[Parameter window = 45 days; prediction magnitude = 16.25; prediction window = 43 days]

Figure 3.20 Values of beta, C and N in each parameter window (entire mine)



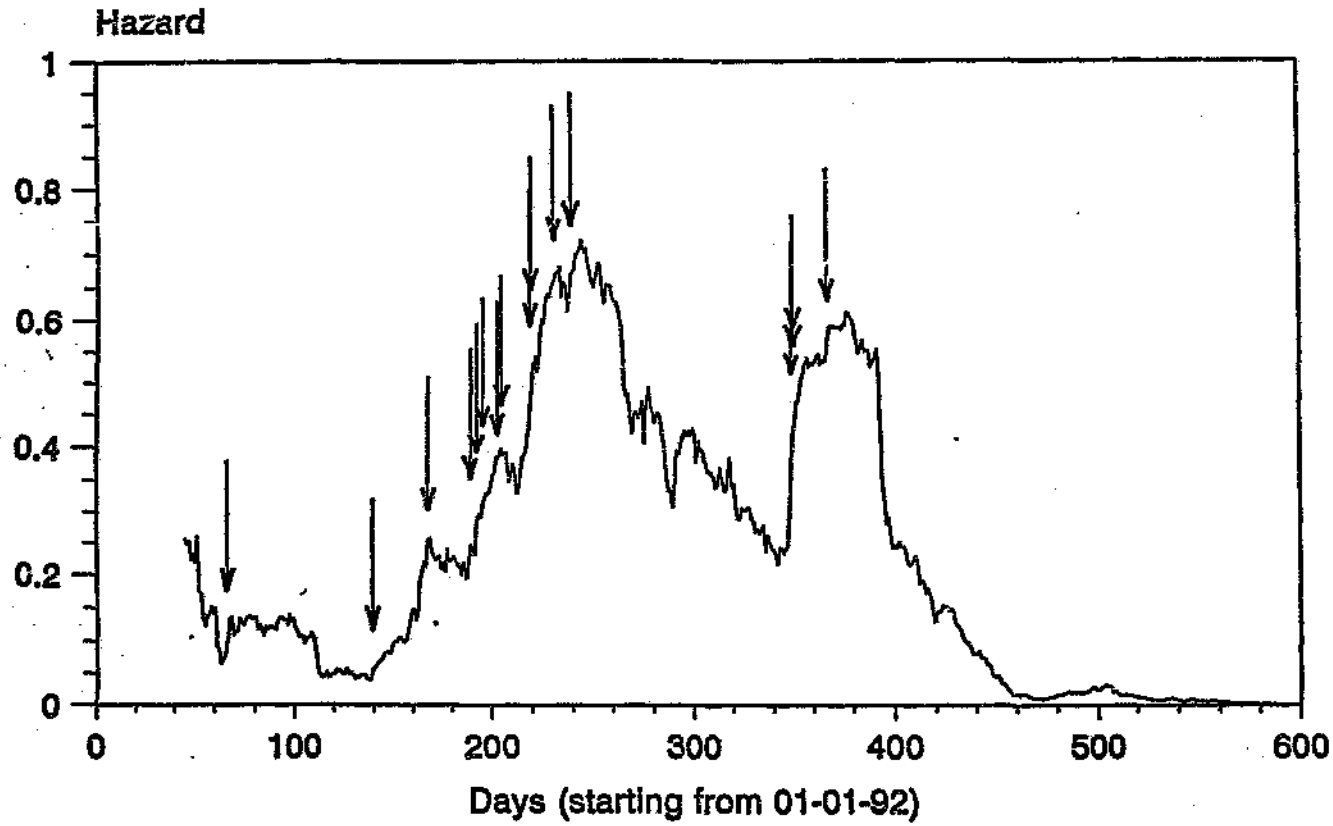
[Parameter window = 12 days; prediction magnitude = 15.... prediction window = 7 days]

Figure 3.21 Seismic hazard (entire mine)



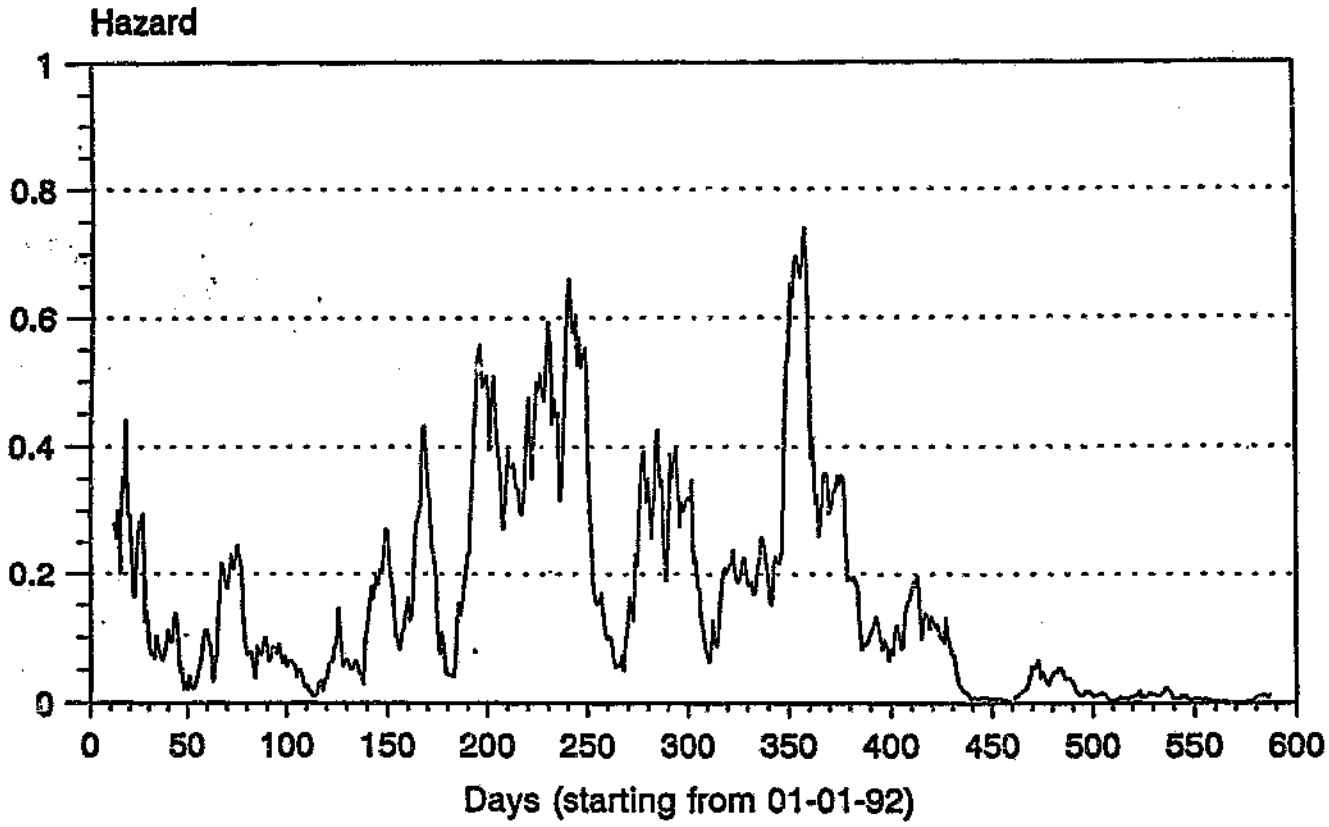
[Parameter window = 30 days; prediction magnitude = 16.00; prediction window = 20 days]

Figure 3.22 Seismic hazard (entire mine)



[Parameter window = 45 days; prediction magnitude = 16.25; prediction window = 43 days]

Figure 3.23 Seismic hazard (entire mine)



[Parameter window = 12 days; prediction magnitude = 15.50; prediction window = 7 days]

Figure 3.24 Seismic hazard (entire mine) - no "event arrows"

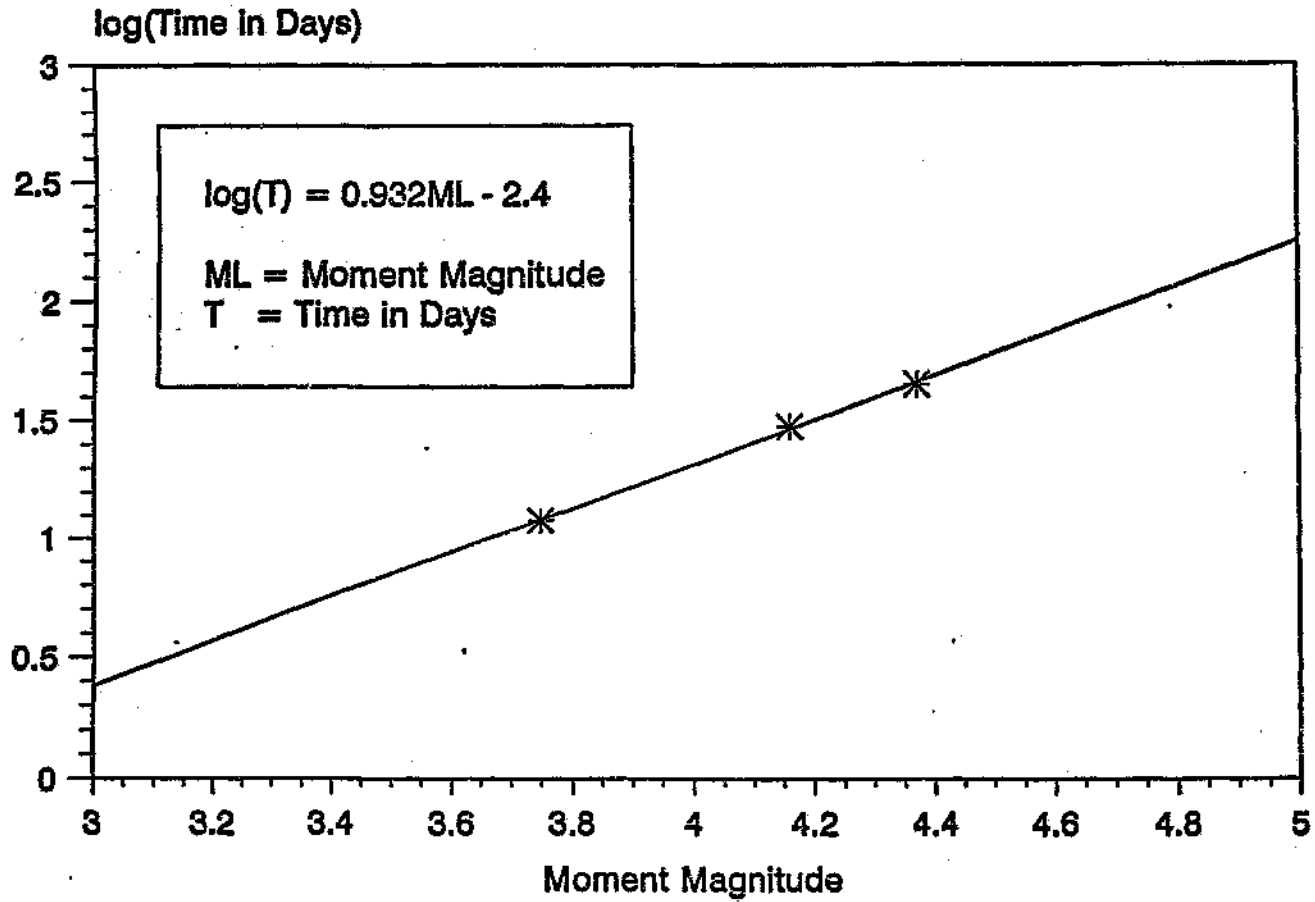


Figure 3.25 Time-magnitude relationship

Chapter 4

DISCUSSION AND CONCLUSION

The usual approach to the statistical analysis of earthquake occurrence rests on two fundamental pillars, viz.

I. The logarithm of the cumulative number of events is a linear function of the magnitude: the so called classical Gutenberg-Richter relationship.

II. The number of earthquakes that occur in an interval of a given size is modelled according to a Poisson distribution.

In our model we have allowed for a non-linear frequency-magnitude relationship, but have retained the premise that the number of events which occur in each time window (parameter window) throughout the catalog is Poissonian.

The implications of the latter are that we tacitly assume the following:

1. Events occur randomly in continuous time

2. Events occur singly

3. Events occur uniformly in time

4. Events occur independently.

By observing Figures (3.18) to (3.20) inclusive, we see that C lies approximately in the range 1.2 to 1.8 and so we are not called upon to justify our assumption of

the non-linearity of the frequency-magnitude relationship. The justification for retaining the Poisson distribution is less clear though, and the results of this project suggest that it should probably be replaced by some non-stationary distribution. (Kijko and Funk, 1993).

Discussion of this model in its relation to cluster size and prediction magnitudes.

Refer to Figures (3.20), (3.24) and (3.35).

1. *There seems to be a small but perceptible improvement in results as the cluster size increases.*

Possible explanations

- A swarm of smaller events surround the occurrence of a large event in what are termed fore- and after-shocks. In a cluster containing a relatively few events in total, this swarming effect can be a dominating feature, and so the events cannot be said to be occurring at random. In large clusters however - the entire mine e.g. - we have the union of a large number of these small clusters, resulting in the occurrence of the events tending to approximate more closely a random process.

- Events do not strictly occur independently: the advent of a large event de-stresses the surrounding rock-mass, making less likely the occurrence of another large event immediately after the first in the same area. Again, when large regions are taken into account, this effect becomes less important.

- Because of the strong correlation between seismicity in adjacent mining areas (Kijko, 1993 and Appendix G), the detection of a precursive build-up in one area can manifest itself as the occurrence of an event in an adjacent area, giving rise, erroneously, to a false alarm.

2. *Large prediction magnitudes seem to give better results than smaller ones.*

Possible explanation

- For a seismic event to occur, considerable strain energy must be accumulated in the surrounding rock mass. It is evident that the larger events are a manifestation of a considerably longer period of energy build-up than the smaller ones. It is speculated that blasting can cause premature triggering of an event by say, a day or two. This will therefore be of tremendous consequence to small events whose build-up times are several days to a week or so, but will be of no consequence to those larger events whose build-up time span several months or more.

At first sight, it may seem advantageous that the model works best for the mine as a whole, the idea being that we can do everything at once. This is not so. To see why not, consider the meaning of prediction in our context. It means giving the *time*, *place* and *magnitude* of an event to come. We contend that this model does not fair badly with respect to the "time" and to the "magnitude", but fails in respect of the "where". It seems obvious that in order to succeed with the location of a predicted event, one must have a model which is successful in the domain of small spatial clusters.

Conclusions

- Indications are that retaining the Poisson distribution will not give rise to models that work well with small localized clusters and the prognosis is bleak that a stationary model will ever be successful for the purpose of prediction in the true sense of the word as outlined above. For areas the size of an entire mine and for moment magnitudes not smaller than say 4.0, the model gives good results, and for reef planes, the results are only a little less good. Far from causing despair, this is extremely encouraging, for it means that we are on the right path and we hope that successive refinements (e.g. replacing the Poisson distribution with a Weibull distribution), of this model will lead ever closer to useful predictive capabilities.

- It is clear that the method of obtaining clusters is also going to have to be refined. Visual identification, as done in this project, seems to offer little by way of sophistication. As mentioned earlier, ISS International have tried space-time clustering techniques (see Appendix D for an outline of this strategy). The new discipline of Fractal clustering will probably also have to be looked into.

Discussion of this model in its relation to parameter and prediction window durations.

One of the things that became evident during the course of this research, was that the duration of the parameter window was of critical importance. The duration of the prediction window by contrast, had essentially the effect of moving the entire graph up or down without much change in shape and was therefore useful in "centralizing" the curve.

We will now attempt to give physical interpretations for the observed changes in the Charts of Fig. (3.8) due to changes in the parameter window duration.

Chart A shows the result of too short a parameter window. A large number of the events occur unexpectedly and the parameter windows are quite often dominated by the large events within them.

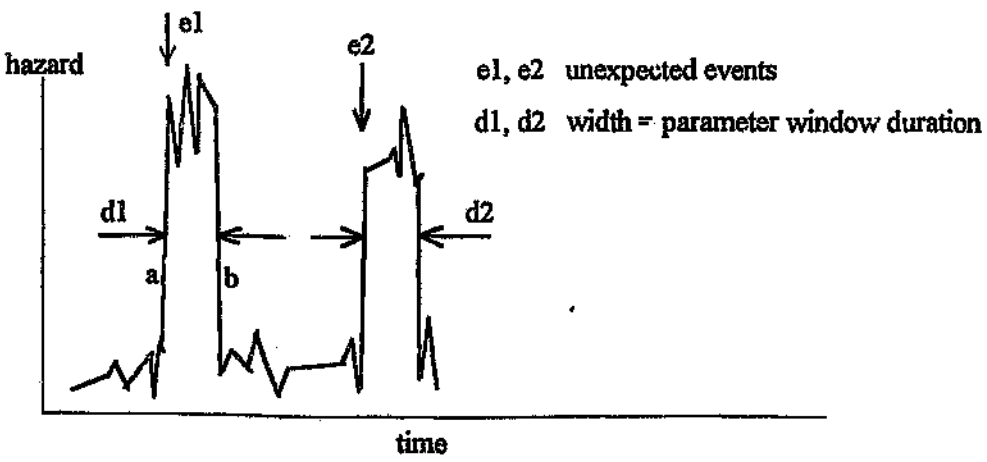


Figure 4.1 The effect of too short a parameter window

By "unexpected event" we mean that the increase in the hazard is a consequence of the occurrence of the large event and not the other way around, as we would prefer.

Mathematically what happens is that when a large event enters this short window (containing few events) it dominates all the other events in the window and the hazard shoots sky-high, as at (a) e.g. in Fig. (4.1). The hazard more or less remains at this level whilst the large event is within the parameter window and then suddenly falls, as at (b) e.g., when the large event exits the parameter window. This is why the duration [a, b] is equal to that of the parameter window.

Physically what is happening, is that the parameter window has a duration which is less than the precursive time necessary to "see" an event with magnitude equal to the given prediction level. That is why it comes upon these unexpectedly. A closer examination of Chart A reveals a multitude of small fluctuations in the probability curve - the model is actually predicting small events commensurate with its window duration.

If, on the other hand, the parameter window duration is too long, excessive smoothing takes place, (mathematically) and the model runs rough-shod over those events having magnitude round about the prediction level, and is trying to locate only the very large events (physically). In this case we can see "unwanted" events in areas where the hazard is consistently low . The ideas presented in this paragraph are depicted in Fig. (4.2) overleaf.

The important thing to realize, is that for a successful hazard analysis, the parameter window duration must be matched to the prediction magnitude.

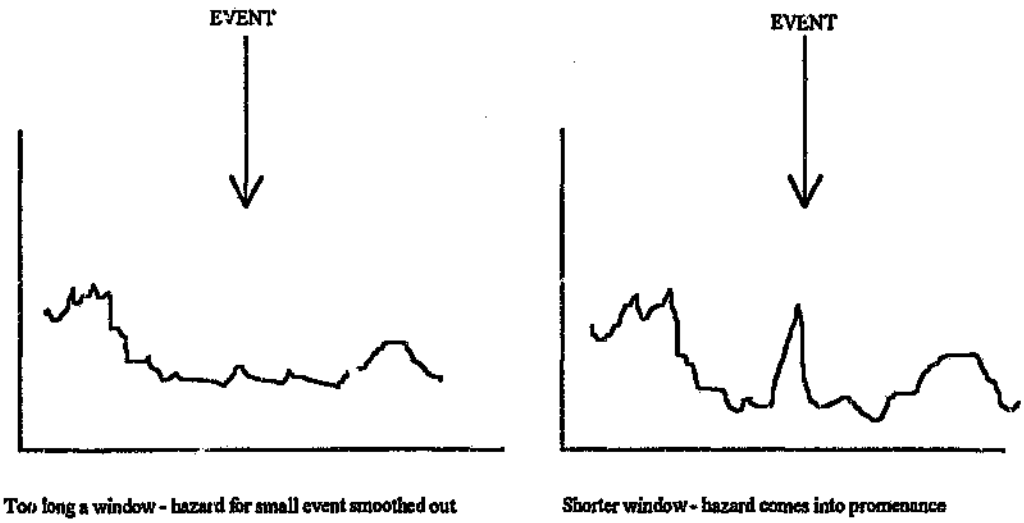


Figure 4.2 A matched window-magnitude pair (right) contrasted with too long a parameter window (left)

Having matched parameter window durations to three different prediction magnitudes as shown in Figures (3.21), (3.22) and (3.23) it was decided to see if an empirical law could be found to fit the magnitude-duration data. Making use of earlier work for natural earthquakes (Tsubokawa, 1969 and 1973), the formula

$$\log(T) = 0.932M_L - 2.4$$

was established, where

T = Precursive Time in Days, and
M_L = Moment Magnitude

Whether T is identical to the energy build-up period commensurate to an event of magnitude M_L is not established; that there exists a significant correlation between the two is probably beyond doubt.

Trying to obtain similar diagrams for magnitudes less than 15.50 and greater than 16.25 has its difficulties. In the former case, the diagram becomes very confused, and in the latter one soon runs into computer capacity problems, e.g. the computer used for this project could not cope with an array of more than about 5000 doubles.

APPENDIX A

Magnitude

We have defined magnitude to mean $\log(M_0 + \gamma E)$ where M_0 is the seismic moment, E is the seismic energy, and γ is a constant.

Detailed derivations of seismic moment and radiated energy are beyond the scope of this project. However, some idea of how they may be evaluated from their seismograms is given.

We take it that we have stored on a computer, all samples corresponding to a velocity seismogram.

Seismic Energy

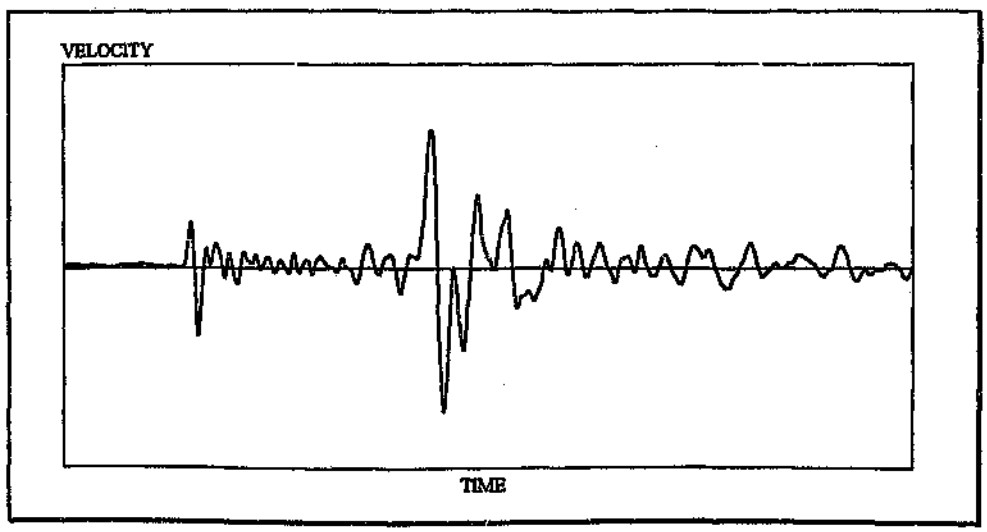


Figure A1 One of the three components of a typical velociy seismogram

We make the following simplifying assumptions:

- we consider the source to be a point.
- the rock-mass is considered both homogeneous and perfectly elastic.
- both P and S waves radiate spherically with equal amplitude in all directions.

Assume the velocity seismogram was obtained from a sensor situated a distance r from the seismic source.

Consider an infinitesimal shell of radius r centred about the source. As the wave-train passes through this shell, it is set in motion. Let us assume that the P wave arrival at the shell occurs at time T_1 and that the S wave departs from the shell at time T_2. The speed of the shell at any time t is given by the corresponding amplitude of the velocity seismogram $v(t)$. The shell has, at any time t, an infinitesimal energy $dE(t)$, composed of kinetic energy $dE_k(t)$ and elastic potential energy $dE_p(t)$.

$$\int_{T_1}^{T_2} dE(t) = \int_{T_1}^{T_2} dE_k(t) + \int_{T_1}^{T_2} dE_p(t) = 2\int_{T_1}^{T_2} dE_k(t)$$

since, for free elastic oscillations, the average kinetic energy equals the average potential energy, and the above integration extends over more than one cycle of the lowest frequency component. Now

$dE_k(t) = 2\pi r^2 \rho V v^2(t) dt$ where Vdt is the thickness of the infinitesimal shell and ρ is the density of the rock, so that

$$E = 4\pi\rho r^2 V \int_{T_1}^{T_2} v^2 dt$$

Seismic Moment

Seismic moment is defined as being equal to $\mu \bar{u} A$ where μ is the modulus of rigidity, $\bar{u}$ is the average slip and A is the area of the fault. (Aki and Richards, 1980 p49).

However, the above definition cannot be used directly to calculate the moment on a computer because A and $\bar{u}$ are unknown. We therefore have to approach the problem from a different direction. One way to do this is to take the FFT of the velocity seismogram, the code to implement this on a computer being given e.g. by McGillem & Cooper, 1991, and then using the fact that the Fourier transform of the integral of a function is $(i2\pi f)^{-1}$ times the Fourier transform of the function, we in effect land up with the Fourier transform of the *displacement* seismogram.

Recovering the underlying continuous function from the transformed data, and then plotting the logarithm of the amplitude against the logarithm of the frequency we end up with the *displacement spectral density*.

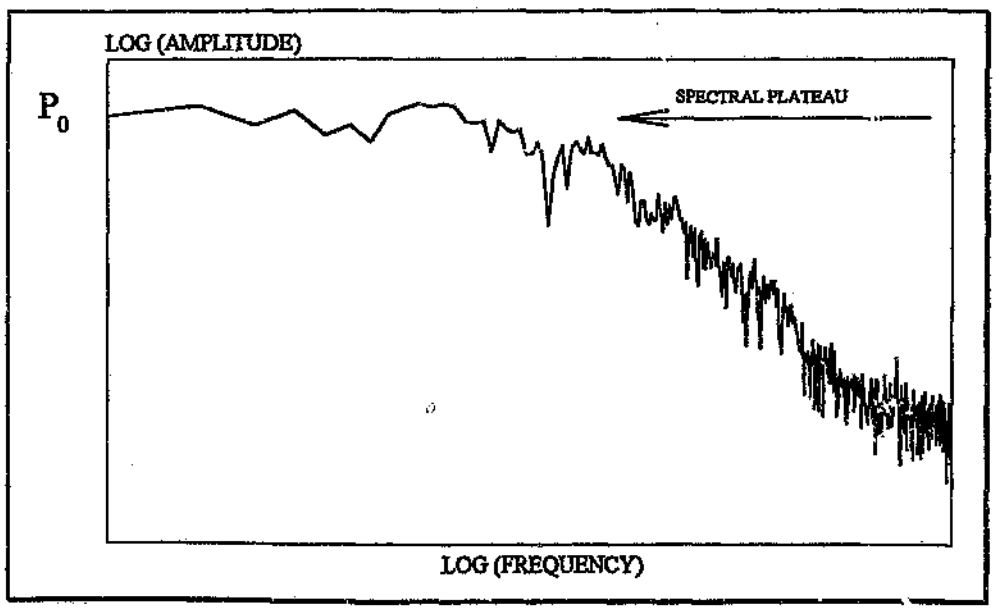


Figure A2 Displacement spectral density of the seismogram shown in Fig. A1

If we assume a *far field* approximation, we can obtain the height P_0, of the so-called *spectral plateau* of the density, since it is just the value of the function as the frequency tends to zero; and since the function in this case is just the Fourier transform of the displacement function $u(t)$, say, we can write e.g.

$$P_0 = \int_{-\infty}^{\infty} u(t)\exp(-i\omega t)dt \Big|_{\omega=0} = \int_{-\infty}^{\infty} u(t)dt \,, \quad \text{where } \omega \text{ is the circular frequency.}$$

From Equation (4.32) on page 81 of Aki and Richards, 1980 , we get with a little modification

$$u(t) = \frac{1}{4\pi\rho V_P^3} A^{FP} \frac{1}{r}\frac{dM_0^{(n)}}{dt} + \frac{1}{4\pi\rho V_S^3} A^{FS} \frac{1}{r}\frac{dM_0^{(n)}}{dt}$$

where we have ignored all but the far-field terms. Integrating both sides w.r.t t and substituting P_0 for the integral on the L.H.S.

$$P_0 = \frac{A^{FP}}{4\pi\rho V_P^3 r} M_0^{(n)} + \frac{A^{FS}}{4\pi\rho V_S^3 r} M_0^{(n)}$$

where r is the source-receiver distance, ρ is the mass-density of the rock, V_P and V_S are the P-wave and S-wave velocities respectively, and A^{FP} and A^{FS} are the far-field P and S radiation patterns respectively.

The above equation is usually written in the more familiar and compact form

$$M_0 = \frac{4\pi\rho V^3 r P_0}{\bar{\xi}_{\theta\phi}}$$

where V stands for either P or S wave velocity ($\approx$ 5900 ms^{-1} and 3400 ms^{-1} respectively) and $\bar{\xi}_{\theta\phi}$ represents either the P or S far-field radiation pattern and has average value equal to approximately 0.39 for P waves and 0.57 for S waves. $\rho \approx 2700$ $kg.m^{-3}$.

Since all values are now known, M_0 can be determined.

Magnitude

From a practical point of view, no single parameter seems to be adequate in describing fully what one intuitively feels about the 'size', of an earthquake. Our "gut-feeling" tells us that the size of a seismic event should take into account the 'amount' of displacement that took place and the 'violence' with which this displacement happened.

The inadequacy of a single parameter arises from the fact that the two processes described above are quite independent of one another; i.e. it is possible to have a large amount of rock movement taking place very gradually on e.g. a 'soft' fault, resulting in a large seismic moment and a small event energy. On the other hand, a small, but violent movement can take place on a 'stiff' fault e.g. , and this will result in a large amount of radiated energy, but small seismic moment.

To overcome this inadequacy, it seems natural to measure the size of an event as a combination of moment and energy, and this is what has indeed been done in our case. It remains only decide upon the weighting in this combination. In view of no good argument to the contrary, we choose equal weighting and therefore write

$\gamma = \sum M_0 \cdot \left[\sum E\right]^{-1}$ where the sums are taken over all representative events in a cluster.

It is an empirical result that in a large majority of cases, the logarithm of the quantity $M_0 + \gamma E$ is exponentially distributed over the minimg operation. Because of our familiarity with this distribution, and because it crops up fairly frequently in our application, we have decided to adopt our definition of magnitude as being equal to $\log(M_0 + \gamma E)$.

For those more accustomed to *moment magnitude* M_L , we derive a rough relationship between it and our rather unconventional definition of magnitude x. From Spottiswoode and McGarr (1975), we have

$\log M_0 = 17.7 + 1.2M_L$ where M_0 is in dyne cm.

Because of the way in which we have chosen γ, we can write

$$x = \log(2M_0)$$

Combining these two equations leads to

$$M_L = \frac{x - 11}{1.2}$$

Table E1 Conversion from magnitude (x) to moment magnitude (M_L)

x	M_L	x	M_L
12.00	0.83	14.75	3.13
12.25	1.04	15.00	3.33
12.50	1.25	15.25	3.54
12.75	1.46	15.50	3.75
13.00	1.67	15.75	3.96
13.25	1.88	16.00	4.17
13.50	2.08	16.25	4.38
13.75	2.29	16.50	4.58
14.00	2.50	16.75	4.79
14.25	2.71	17.00	5.00
14.50	2.92	17.25	5.21

APPENDIX B

Sufficiency Conditions for Maxima

Let us write $L^*(\beta, C) = \ln L(\beta, C)$ for convenience and consistency with Chapter 2.

We have already noted that in order for $L^*(\beta, C)$ to have a maximum value for $\beta = \hat{\beta}$, $C = \hat{C}$, it is necessary that for these values (e.g. Woods, 1954).

$$\frac{\partial L^*(\beta, C)}{\partial \beta} = 0, \quad \frac{\partial L^*(\beta, C)}{\partial C} = 0.$$

However, all we really have at this stage is that $\hat{\beta}$ and $\hat{C}$ are *stationary* values of L^*. We do not know whether these values maximize or minimize L^* or indeed if L^* has a maximum or minimum at all.

To settle this matter, it is a *sufficient* condition for L^* to have a maximum or a minimum, if $\frac{\partial^2 L^*}{\partial \beta^2}\frac{\partial^2 L^*}{\partial C^2} - \left(\frac{\partial^2 L^*}{\partial \beta \partial C}\right)^2 > 0$ at the critical values. (B.1)

If Inequality (B.1) is true, and in addition $\frac{\partial^2 L^*}{\partial \beta^2} < 0$ and $\frac{\partial^2 L^*}{\partial C^2} < 0$ then L^* has a **maximum** value at the critical values of the variables.

We can easily verify that the latter two conditions hold, remembering that $\hat{\beta} > 0$ and $\hat{C} \geq 1$ on physical grounds, and of course $(x_1 - x_0) \geq 0$, by hypothesis.

$$\left.\frac{\partial^2 L^*}{\partial \beta^2}\right|_{\hat{\beta}} = -\frac{n}{\hat{\beta}^2} < 0 \text{ and}$$

$$\left.\frac{\partial^2 L^*}{\partial C^2}\right|_{\hat{C}} = -\left\{\frac{n}{\hat{C}^2} + \hat{\beta}\sum (x_i - x_0)^{\hat{C}} [\ln(x_i - x_0)]^2\right\} < 0$$

It remains only to show that the inequality (B.1) holds.

From the Schwarz inequality we have

$$\sum (x_i - x_0)^{2\hat{C}} [\ln(x_i - x_0)]^2 \geq \left[\sum (x_i - x_0)^{\hat{C}} \ln(x - x_0)\right]^2 \qquad \text{(B.2)}$$

If $b = 1$, then about 90% of all events reside in the magnitude interval x_0 to x_0+1. This being the case, then 90% of the terms in the series

$$(x_1 - x_0)^{\hat{C}} [\ln(x_1 - x_0)]^2 + (x_2 - x_0)^{\hat{C}} [\ln(x_2 - x_0)]^2 + \cdots + (x_n - x_0)^{\hat{C}} [\ln(x_n - x_0)]^2$$

have increased their value as compared to the series

$$(x_1 - x_0)^{2\hat{C}} [\ln(x_1 - x_0)]^2 + (x_2 - x_0)^{2\hat{C}} [\ln(x_2 - x_0)]^2 + \cdots + (x_n - x_0)^{2\hat{C}} [\ln(x_n - x_0)]^2$$

since about 90% of the terms $(x_k - x_0)^{\hat{C}} < 1$. This means that we can re-write Inequality (B.2) as

$$\sum (x_i - x_0)^{\hat{C}} [\ln(x_i - x_0)]^2 \geq \left[\sum (x_i - x_0)^{\hat{C}} \ln(x - x_0)\right]^2 \qquad \text{(B.3)}$$

In general, this argument is weak, since the 10% that decrease in value may dominate the others. However, *we now insist that* (B.3) *hold*, deeming inadmissible those data sets for which the inequality is violated. [1]

Because n $>> \hat{\beta}$, it follows that

$$\left(\frac{n}{\hat{\beta}\,\hat{C}}\right)^2 + \frac{n}{\hat{\beta}}\sum (x_i - x_0)^{\hat{C}} [\ln(x_i - x_0)]^2 > \left[\sum (x_i - x_0)^{\hat{C}} \ln(x_i - x_0)\right]^2$$

and since the right hand side of the inequality equals $\left(\frac{\partial^2 L^*}{\partial \beta \partial C}\right)^2\Big|_{\hat{\beta};\hat{C}}$ it follows that inequality (B.1) holds.

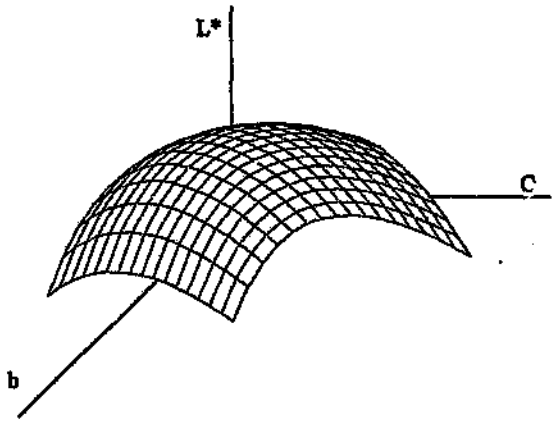


Figure B1 Mesh of (the logarithm of) the likelihood function for typical values of the parameters

[1] It must be pointed out that this is hardly any restriction at all for the application at hand and (B.3) will hold in the overwhelming majority of cases. In fact it is difficult to see how it could be violated , for then b would have to be unrealistically small.

APPENDIX C

The Poisson Process

The following is adapted from Cox and Lewis (1966).

Let us consider events occurring singly along a time axis and let λ be a constant which measures the mean rate of occurrence of these events over a long period of time. Further, let $N(\cdot)$ be the random variable which assigns to each time period $(t, t+h]$, the number of events which occurred in it.

Suppose that as $h \to 0$;

i) $P_r[N(h) = 1] = \lambda h + o(h)$

ii) $P_r[N(h \geq 2] = o(h)$

iii) and that the number of events in non-overlapping time intervals are independent,

then $N(\cdot)$ is said to have a Poisson distribution, and for any arbitrary interval of length Δt, it can be shown that

$$P_r[N(\Delta t) = n] = \frac{(\lambda \Delta t)^n e^{-\lambda \Delta t}}{n!} \quad n = 0, 1, 2, \cdots \qquad \text{(C.1)}$$

Since the Poisson process has no memory, the probability that no event occurs in any time interval Δt, after a time t has elapsed, i.e. in the interval $(t, t+\Delta t)$ is, from (C.1), simply $P_r[N(\Delta t) = 0] = \exp(-\lambda \Delta t)$. This means that at least one event occurring in this interval is given by

$$P_r[N(\Delta t) \geq 1] = 1 - \exp(-\lambda \Delta t)$$

We notice therefore, that times between seismic events are distributed exponentially.

APPENDIX D

Space -Time Clustering

General description

The technique used here is a modified version of the *single-link cluster analysis* (SLC) used by Matsumura (1984), Frohlich and Davis (1990), and Davis and Frohlich (1991).

Suppose the entire database contains N events. The procedure begins by linking each event to its nearest neighbour. At this stage we have between N/2 and N-1 links. Now, each group thus formed, is linked to its nearest neighbouring group. This process is repeated until there are N-1 links, at which stage the procedure terminates. All links which are longer than some specified value are now removed. If this resulted in the removal of k links, we would be left with k+1 clusters.

For the present application the above method of obtaining clusters is not practical because it would be too time consuming. A piecemeal procedure (Kijko, et al., 1993) has therefore been adopted, whereby a moving time window of some specified length traverses the database. (This must not be confused with the parameter or prediction windows mentioned earlier).

For each new event that comes into the window, link lengths begin being calculated between this most recent event and all the other events already in the window. As soon as a link is found that is less than the maximum link length allowed, the two events are joined together, with the restriction that only one link is allowed to form between two events which both belong to the same cluster. Therefore, these events are not necessarily nearest neighbours.

At some stage in the clustering process, an event from one cluster may link to an event belonging to another cluster: the program will then merge the two clusters. Occasionally, two clusters should have been linked together, but no events occurred close enough to each other for a link to have been established. This situation can arise e.g. from using a time window which is not long enough. This problem is overcome by having the program periodically check the distance between cluster centroids, and if they fall below some given distance, the program merges the clusters together.

The choice of the window length is important, for if it is too short, it may on occasion contain no events and this would effectively terminate the cluster, whilst if it is too long, it could defeat the purpose of windowing in the first place, and slow down the operation of the process unnecessarily A proper choice of window length depends to a large extent on the average event rate for the mine in question.

Space-time metric

In a cluster of seismic events, we are looking for some sort of *proximity* of these events to one another.

Intuitively, two concepts of proximity spring to mind: (i) events can be close together in time, and (ii), events can be close together in space. Because we have no compelling argument to choose one of these criteria over the other, we endeavour to incorporate them both into our measure of distance. Following the example of Frolich and Davis (1990), we write

$$d_{st} = \sqrt{r^2 + \alpha t^2} \qquad \text{(D.1)}$$

where d_{st} is our space-time inter-event distance, r is the spatial distance between events and t is the time between them.

α is a constant having the units of velocity.

There seems to be no compelling justification for using this so-called Pythagorean form of our metric, save that we feel comfortable with such familiar expressions.

It remains now to determine α. For want of a better suggestion, let us choose it so that the spatial and temporal components contribute equally to d_{ij}. This means that $\sum_{i,j=1}^{N} r_{i,j}^2 = \alpha \sum_{i,j=1}^{N} t_{i,j}^2$ must hold for all N events i, j in some sample deemed to represent the average seismicity on the mine.

APPENDIX E

Program Listings

This appendix lists the main programs used in the project. A lot of programs which simply manipulate the data e.g. change YYMMDDhhmm to YY MM DD hh mm (where, as usual, YY stands for year and MM for month etc.), or those which perform very simple tasks, are not shown. Programs which are adaptations of other programs specifically written for this project are similarly not shown, while some of the listed programs have been abbreviated. This is felt to be in keeping with the fact that this is essentially *not* a programming project.

Comments have been progressively eliminated: this means that they are given the first time that a new feature appears and are then eliminated when the feature appears again in the same or later programs.

Programs E. 1 and E. 8 below, were not specifically written for this project and in fact were written some two years before the commencement of this project. All remaining programs were written specifically for this project, and *all* programs were written by myself, albeit adapted from other sources in some instances.

An "off the shelf" graphics package has been used to produce the graphs in this project whenever the number of data points is less than 1000, which is a limiting feature of the package.

List and brief action of Programs

E. 1	goldseam.for	- finds the equation of the reef planes.
E. 2	scatr_xy.cpp	- draws a scatter diagram of the events.
E. 3	getclust.cpp	- gets events within a cluster.
E. 4	blasts.cpp	- histogram showing the effect of blasting on event rate.
E. 5	bvals.cpp	- used in obtaining the Gutenberg-Richter relationship.
E. 6	getbevnt.cpp	- lists events bigger than some specified value.
E. 7	evalhazd.cpp	- evaluates the hazard.
E. 8	runtime.h	- a header file for dynamic allocation of arrays.

Listing of program E.1 (adapted from Angell & Griffith, 1989).

```
*+----------------------------+
      program goldseam
*+----------------------------+


* Scheme for a set of variables
*********************************

      implicit none

* Three Points
*-------------

      double precision r1(3), r2(3), r3(3)


* One Plane
*----------

      double precision n1(3), k1


* Indexing variable
*------------------

      integer i


* Initializing the variables
*---------------------------

      do 10 i=1,3
      n1(i)=0.0
      r1(i)=0.0
      r2(i)=0.0
      r3(i)=0.0
10    continue

      k1=0.0



* Getting data
*.............

      print *,'Input the three points one after the other'
      read(*,*) (r1(i), i=1,3),(r2(i), i=1,3),(r3(i), i=1,3)


* Calling the subroutine
*.......................

      call plane(r1,r2,r3,n1,k1)


* Displaying output
*..................

      write(*,20) (n1(i), i=1,3), k1
20    format(//,3x,'(',f12.0,',',f12.0,',',f12.0,').v =',f16.0,//)
```

```
* Ending the run
*...............

      stop
      end


*********************************************************************
      subroutine plane(a,b,c,n,k)
*********************************************************************

* Calculates the vector equation of the plane passing
* through the three points (a(1),a(2),a(3)),
* (b(1),b(2),b(3)) and (c(1),c(2),c(3)).

      implicit none

* Argument declarations
      double precision a(3), b(3), c(3), n(3), k

* Local declarations
      double precision d1(3), d2(3)


      d1(1)=b(1)-a(1)
      d2(1)=c(1)-b(1)
      d1(2)=b(2)-a(2)
      d2(2)=c(2)-b(2)
      d1(3)=b(3)-a(3)
      d2(3)=c(3)-b(3)
      call vecprd(d1,d2,n)
      k=n(1)*a(1)+n(2)*a(2)+n(3)*a(3)
      return
      end



*********************************************************************
      subroutine vecprd(e,f,g)
*********************************************************************

* Calculates the vector product, (g(1),g(2),g(3))
* = (e(1),e(2),e(3)) X (f(1),f(2),f(3)).

      implicit none

* Argument declarations
      double precision e(3), f(3), g(3)


      g(1)=e(2)*f(3)-e(3)*f(2)
      g(2)=e(3)*f(1)-e(1)*f(3)
      g(3)=e(1)*f(2)-e(2)*f(1)
      return
      end
```

Listing of Program E.2

```
/* SCATR_XY.CPP
 *
 * Plots either the VCR or the CL ents in plan and
 * draws in the appropriate boundry.
 */

#include <graphics.h>
#include <stdio.h>
#include <stdlib.h>
#include <conio.h>
#include <math.h>
#include <string.h>

int main(int argc, char **argv){
int gdriver = VGA;
int gmode   = VGAHI;
int errorcode, YY, MM, DD, hh, mm;
int i, x, y, X, Y, XP1, YP1;
float LocX, LocY, LocZ, Xmax, Xmin, Ymax, Ymin, Moment, Energy;
char buffer[40];
char maintitle[80];
char xtitle[20];
char ytitle[20];
char subtitle[80];
FILE *fp;

/*
 * Apices on the boundry for the VCR = (vx[i], vy[i])
 */

float vx[15] = {28000.0, 26412.0, 26480.0, 25275.0, 27000.0,
                27563.0, 27838.0, 28375.0, 29220.0, 30287.0,
                29438.0, 29925.0, 29300.0, 30250.0, 28000.0};

float vy[15] = {-37575.0, -41025.0, -41325.0, -44750.0, -45350.0,
                -44019.0, -44188.0, -43388.0, -43950.0, -42343.0,
                -41800.0, -41085.0, -40650.0, -38825.0, -37575.0};

/*
 * Apices on the boundry for the CL = (cx[i], cy[i])
 */

float cx[10] = {27750.0, 26400.0, 26500.0, 25063.0, 26750.0,
                27000.0, 28738.0, 29613.0, 29788.0, 27750.0};

float cy[10] = {-37263.0, -41075.0, -41375.0, -45425.0, -45900.0,
                -45000.0, -45000.0, -40000.0, -37268.0, -37263.0};


/*
 * Checking Correct Usage
 */

if(argc != 7){
printf("\nUsage: %s [FILENAME][Xmax][Xmin][Ymax][Ymin][V/C]\n",
argv[0]);
exit(0);
}
```

```
/*
 * Getting command line arguments
 */

Xmax = atof(argv[2]);
Xmin = atof(argv[3]);
Ymax = atof(argv[4]);
Ymin = atof(argv[5]);

/*
 * Opening the File for Reading and Reporting any Errors
 */

if((fp = fopen(argv[1], "r")) == NULL){
printf("\nCannot open file.\n");
exit(0);}

/*
 * Going into Hi-Res VGA Mode and initializing font
 */

registerbgidriver(EGAVGA_driver);
registerbgifont(sansserif_font);
initgraph(&gdriver, &gmode, "");

/*
 * Check that Computer can Support Hi-Res VGA (16-Colour) Mode
 */

errorcode = graphresult();
if(errorcode != grOk){
printf("Graphics Function Error: %s\n", grapherrormsg(errorcode));
printf("\nHit any Key to Stop\n");
getch();
exit(1);
}

/*
 * Draw Outer Rectangle
 */

rectangle(0,0,639,479);

/*
 * Various Titles
 */

if(!stricmp(argv[6], "V"))
sprintf(maintitle,"SCATTER DIAGRAM FOR VCR EVENTS");
else
sprintf(maintitle,"SCATTER DIAGRAM FOR CL EVENTS");
sprintf(subtitle,"Period: 01 Jan 92 - 10 Aug 93");
sprintf(xtitle,"Y-Axis");
sprintf(ytitle,"X-Axis");

setcolor(12);
settextstyle(DEFAULT_FONT, HORIZ_DIR, 2);
settextjustify(CENTER_TEXT, CENTER_TEXT);
outtextxy(320, 40, maintitle);
setcolor(11);
outtextxy(320, 70, subtitle);
setcolor(15);
settextstyle(DEFAULT_FONT, HORIZ_DIR, 1);
outtextxy(320, 470, xtitle);
settextstyle(DEFAULT_FONT, VERT_DIR, 1);
outtextxy(10, 220, ytitle);
```

```
/*
 * Draw Inner Rectangle
 */

setcolor(2);
rectangle(60, 90, 620, 440);

/*
 * Set up axes with correct values automatically worked out
 */

setcolor(15);
settextstyle(DEFAULT_FONT, HORIZ_DIR, 1);
settextjustify(RIGHT_TEXT, CENTER_TEXT);

sprintf(buffer, "%5.0f", Xmin);
outtextxy(55,90, buffer);

sprintf(buffer, "%5.0f", 0.25*Xmax + 0.75*Xmin);
outtextxy(55, 178, buffer);

sprintf(buffer, "%5.0f", 0.5*(Xmax + Xmin));
outtextxy(55, 265, buffer);

sprintf(buffer, "%5.0f", 0.75*Xmax + 0.25*Xmin);
outtextxy(55, 353, buffer);

sprintf(buffer, "%5.0f", Xmax);
outtextxy(55, 440, buffer);

settextjustify(CENTER_TEXT, TOP_TEXT);

sprintf(buffer, "%6.0f", Ymin);
outtextxy(610, 450, buffer);

sprintf(buffer, "%6.0f", 0.75*Ymin + 0.25*Ymax);
outtextxy(480, 450, buffer);

sprintf(buffer, "%6.0f", 0.5*(Ymin + Ymax));
outtextxy(340, 450, buffer);

sprintf(buffer, "%6.0f", 0.25*Ymin + 0.75*Ymax);
outtextxy(200, 450, buffer);

sprintf(buffer, "%6.0f", Ymax);
outtextxy(60, 450, buffer);

/*
 * Read the x, y, and z locations of events from the file
 */

while(fscanf(fp,"%d %d %d %d %d %f %f %f %e %e",
&YY, &MM, &DD, &hh, &mm, &LocX, &LocY, &LocZ, &Moment, &Energy) !=
EOF){

/*
 * Select only those events within the chosen area and make
 * sure that they all fit into the work-space
 */

if(!stricmp(argv[6], "V")){
if(LocX >= Xmin && LocX <= Xmax && LocY >= Ymin && LocY <= Ymax
&& LocZ >= 500.0 && LocZ <= 0.34657*LocX - 0.14175*LocY -
12943.5){
x = (int) (60.0 + 560.0*((Ymax - LocY)/(Ymax - Ymin)));
y = (int) (90.0 + 350.0*((LocX - Xmin)/(Xmax - Xmin)));
```

```
putpixel(x, y, 14);
}
}
else
if(LocX >= Xmin && LocX <= Xmax && LocY >= Ymin && LocY <= Ymax
&& LocZ > 0.34657*LocX - 0.14175*LocY - 12943.5 && LocZ < 0.3878
*LocX - 0.0353*LocY - 8665.5){
x = (int) (60.0 + 560.0*((Ymax - LocY)/(Ymax - Ymin)));
y = (int) (90.0 + 350.0*((LocX - Xmin)/(Xmax - Xmin)));
putpixel(x, y, 14);
}
}

/*
 * Draw in the appropriate boundry
 */

setlinestyle (SOLID_LINE, 0xFFFF, THICK_WIDTH);
setcolor(4);
if(!stricmp(argv[6], "V")){
for(i=0;i<14;i++){
X = (int) (60.0 + 560.0*((Ymax - vy[i])/(Ymax - Ymin)));
XP1 = (int) (60.0 + 560.0*((Ymax - vy[i+1])/(Ymax - Ymin)));
Y = (int) (90.0 + 350.0*((vx[i] - Xmin)/(Xmax - Xmin)));
YP1 = (int) (90.0 + 350.0*((vx[i+1] - Xmin)/(Xmax - Xmin)));
line(X, Y, XP1, YP1);
}
}
else
for(i=0;i<9;i++){
X = (int) (60.0 + 560.0*((Ymax - cy[i])/(Ymax - Ymin)));
XP1 = (int) (60.0 + 560.0*((Ymax - cy[i+1])/(Ymax - Ymin)));
Y = (int) (90.0 + 350.0*((cx[i] - Xmin)/(Xmax - Xmin)));
YP1 = (int) (90.0 + 350.0*((cx[i+1] - Xmin)/(Xmax - Xmin)));
line(X, Y, XP1, YP1);
}



/*
 * Hit any Key to Return Screen to Text Mode
 */

getch();
closegraph();
return 0;
}



/* Note:    The output of this - and similar - programs have been
 *          altered slightly to conform as far as possible to
 *          Rule 5.4 in the "Guide for the preperation of Theses,
 *          Dissertations and Project Reports".
 */
```

Listing of Program E.3

The ideas used in this program are to be found in Angell and Griffith (1989).

```
/* GETCLUST.CPP
 *
 * This program scanns through the data and decides which events
 * are inside and which are outside a given Polygon which in this
 * case delineates the chosen cluster. The chosen events are
 * written to a file. The user must specify if the VCR or CL is
 * being processed.
 *
 * Return value for function inside(float,float,float*,float*,int);
 *-----------------------------------------------------------------
 *    0 if the point is on the edge or inside the polygon
 *    Some positive integer otherwise.
 *-----------------------------------------------------------------
 */

#include <stdio.h>
#include <stdlib.h>
#include <string.h>
#include <math.h>
#include "runtime.h"

int inside(float ix, float iy, float *px, float *py, int size);

void main(int argc, char **argv){

FILE *pi, *po;

float YY, MM, DD, hh, mm, LocX, LocY, LocZ,
      Moment, Energy, *Px, *Py;

int   i, N;

if(argc != 4){
printf("\nUsage:%s [Input File][Output File][V or C]\n", argv[0]);
exit(0);
}

if((pi = fopen(argv[1], "r")) == NULL){
printf("\nCannot open file %s\n", argv[1]);
exit(0);
}

if((po = fopen(argv[2], "w")) == NULL){
printf("\nCannot create file %s\n", argv[2]);
exit(0);
}

printf("\nHow many apices in the CLOSED polygon eg triangle = 4");
scanf("%d", &N);

DIM1(Px, N, float);
DIM1(Py, N, float);      /* see runtime.h for details */

printf("\nEnter x and y values of each of the %d apices\n", N);
printf("\none after the other in order without punctuation\n");
for(i=0;i<N;i++)
scanf("%f %f", &Px[i], &Py[i]);
```

```
while (fscanf(pi,"%f %f %f %f %f %f %f %e %e", &YY, &MM, &DD,
&hh, &mm, &LocX, &LocY, &LocZ, &Moment, &Energy) != EOF){
if(!stricmp(argv[3], "v")){
if(!inside(LocX, LocY, Px, Py, N) &&
LocZ > 500.0 && LocZ <= 0.34657*LocX - 0.14175*LocY - 12943.5)
fprintf(po,"%2.0f %2.0f %2.0f %2.0f %2.0f %7.0f %7.0f %6.0f %e
e\n",
YY, MM, DD, hh, mm, LocX, LocY, LocZ, Moment, Energy);
}
else if(!inside(LocX, LocY, Px, Py, N) &&
LocZ > 0.34657*LocX - 0.14175*LocY - 12943.5 && LocZ < 0.3878*LocX
- 0.0353*LocY - 8665.5)
fprintf(po,"%2.0f %2.0f %2.0f %2.0f %2.0f %7.0f %7.0f %6.0f %e
%e\n",
YY, MM, DD, hh, mm, LocX, LocY, LocZ, Moment, Energy);
}
fclose(pi);
fclose(po);
}

int inside(float ix, float iy, float *px, float *py, int size){
int i, k = 0;
for(i=0; i<size-1; i++)
if((px[i+1]-px[i])*(iy-py[i])-(py[i+1]-py[i])*(ix-px[i]) < 0)
k++;
return(k);
}
```

Listing of Program E.4

```
/* BLASTS.CPP
 *
 * This program finds the number of events per day averaged over
 * the entire catalog, in each of the 24 hourly intervals in a
 * day.
 */

#include <stdio.h>
#include <stdlib.h>
#include <string.h>
#include <math.h>

void main(int argc, char *argv[]){

FILE *InFile;

double Moment, Energy, Xco;
int A[24], YY, MM, DD, hh, mm, i;
float LocX, LocY, LocZ;

for(i=0;i<24;i++) A[i] = 0;

if(argc != 3){
printf("\nUsage: [Input File][Cutoff Magnitude]\n");
exit(0);
}

if((InFile = fopen(argv[1], "r")) == NULL){
printf("\nCannot open file %s\n", argv[1]);
exit(0);
}

Xco = atof(argv[2]);
```

```
while (fscanf(InFile,"%d %d %d %d %d %f %f %f %le %le",
&YY, &MM, &DD, &hh, &mm, &LocX, &LocY, &LocZ, &Moment, &Energy) !=
EOF){
if(log10(Moment + 36265.6*Energy) >= Xco){
if(hh >= 0  && hh < 1)  A[0] += 1;
if(hh >= 1  && hh < 2)  A[1] += 1;
if(hh >= 2  && hh < 3)  A[2] += 1;
 .  .  . .   .    . .     .   . .
 .  .  . .   .    . .     .   . .

if(hh >= 23 && hh < 24) A[23] += 1;
}
}
for(i=0;i<24;i++)
printf("%d:30 %8.3f\n", i, ((float)A[i])/587.5);
fclose(InFile);
}
```

Listing of Program E.5

```
/* BVALS.CPP
 *
 * This program groups Magnitude into 0.25 class intervals.
 *
 * It then takes the log of the cumulative frequency in each
 * interval and prints out a magnitude-frequency table that can be
 * used to draw the Gutenberg-Richter curve.
 */

#include <stdio.h>
#include <stdlib.h>
#include <string.h>
#include <math.h>

void main(int argc, char *argv[]){

FILE *InFile;
double A[72], B[73];
float Minutes, Magnitude, LMoment, LEnergy;
int i, j;

for(i=0;i<72;i++){
A[i] = 0.0;
B[i] = 0.0;
}
B[72] = 0.0;

if(argc != 2){
printf("\nUsage: [Input File]\n");
exit(0);
}

if((InFile = fopen(argv[1], "r")) == NULL){
printf("\nCannot open file %s\n", argv[1]);
exit(0);
}

while (fscanf(InFile,"%f %f %f %f",
&Minutes, &Magnitude, &LMoment, &LEnergy) != EOF){
```

```
if(Magnitude >= 7.00  && Magnitude < 7.25)  A[0] += 1.0;
if(Magnitude >= 7.25  && Magnitude < 7.50)  A[1] += 1.0;

 .    .    .   .   .    .   .   .    .   .   .
 .    .    .   .   .    .   .   .    .   .   .
 .    .    .   .   .    .   .   .    .   .   .

if(Magnitude >= 24.75 && Magnitude < 25.00) A[71] += 1.0;
}

for(i=71;i>=0;i--) B[i] = A[i] + B[i+1];

i = 0;

while(B[i] > 0.0){
B[i] = log10(B[i]);
i++;
}
for(j=0;j <= i;j++)
printf("%8.3f %9.4lf\n", 7.125 + (float)j*0.25, B[j]);

fclose(InFile);
}
```

Listing of Program E.6

```
/* GETBEVNT.CPP
 *
 * The purpose is to find the BIG EVENTS having Mag above X.
 *
 * This program acts on the data and evaluates the date to the
 * nearest day (starting 52 minutes after midnight on January 1,
 * 1992) and also combines Moment and Energy into Magnitude, using
 * the value of gamma obtained from GAMAMET.EXE.
 */

#include <stdio.h>
#include <stdlib.h>
#include <string.h>
#include <math.h>

void main(int argc, char *argv[]){

FILE *InFile, *OutFile;

float YY, MM, DD, hh, mm, m, Days, LocX, LocY, LocZ;
double Moment, Energy, g, X, Magnitude;
m = 0.0; Magnitude = 0.0;
if(argc != 5){
printf("\nUsage: [Input File] [Out File] [gamma][X]\n");
exit(0);
}

g = atof(argv[3]);
X = atof(argv[4]);

if((InFile = fopen(argv[1], "r")) == NULL){
printf("\nCannot open file %s\n", argv[1]);
exit(0);
}

if((OutFile = fopen(argv[2], "w")) == NULL){
printf("\nCannot create file %s\n", argv[2]);
exit(0);
}
```

```
while (fscanf(InFile,"%f %f %f %f %f %f %f %le %le",
&YY, &MM, &DD, &hh, &mm, &LocX, &LocY, &LocZ, &Moment, &Energy) !=
EOF){

if(YY == 92){
             if(MM == 1)  m = 0.0;
             if(MM == 2)  m = 31.0;
             .  .   . .   . .   .
             .  .   . .   . .   .

             if(MM == 12) m = 335.0;
            }

if(YY == 93){
             if(MM == 1)  m = 366.0;
             if(MM == 2)  m = 397.0;
             .  .   . .   . .   .
             .  .   . .   . .   .

             if(MM == 8)  m = 578.0;
            }

if(hh < 12.0) Days = m + (DD-1.0);
else          Days = m + DD;
Magnitude = log10(Moment + g*Energy);

if(Magnitude >= X)
fprintf(OutFile,"%8.0f %8.4lf\n", Days, Magnitude);
}

fclose(InFile);
fclose(OutFile);
}
```

Listing of Program E.7

```
/* EVALHAZD.CPP
 *
 * A program to find the value of the Hazard (H) using a modified
 * false position algorithm (Nakamura 1993) to find the value of
 * C.
 * The values of H are written to a user specified file and can be
 * plotted using a commercial graphics package.
 */

#include <stdio.h>
#include <stdlib.h>
#include <math.h>
#include "runtime.h"
double f(double q, int n, double *P);
double BV(double cee, int numb, double *Mag);

void main(int argc, char *argv[]){

FILE *InFile, *OutFile;

double **HAZ, *X, Magnitude, dD, dN, ar, Lower, Upper,
       dParmwind, xm, Ya, Yb, Yc, a, b, c, CC, Cutoff;

float Minutes, j;
int h, i, D, N, k, KR, KL, IL, t, NPW, Parmwind;

if(argc != 3){
printf("\n%s>[In File][Out File]\n", argv[0]);
exit(0);}
```

```
printf("\nCutoff Magnitude (= Xo - 0.125):\n"); /* Utsu (1971) */
scanf("%lf", &Cutoff);
printf("\nMaximum Number of Iterations:\n");
scanf("%d", &IL);
printf("\nConvergence Criteria:\n");
scanf("%lf", &CC);
printf("\nLower Interval Limit:\n");
scanf("%lf", &Lower);
printf("\nUpper Interval Limit\n");
scanf("%lf", &Upper);
printf("\nMaximum Number of Events in Parameter Window\n");
scanf("%d", &NPW);
printf("\nPrediction Time in Days:\n");
scanf("%d", &D);
printf("\nPrediction Magnitude Xm:\n");
scanf("%lf", &xm);
printf("\nDuration of Parameter Window - in Days\n");
scanf("%d", &Parmwind);
if((OutFile = fopen(argv[2], "w")) == NULL){
printf("\nCannot create file %s\n", argv[2]);
exit(0);
}
DIM1(X, NPW, double);
DIM2(HAZ, (588 - Parmwind), 4, double);

for(i=0;i<(588 - Parmwind);i++) for(h=0;h<4;h++)  HAZ[i][h] = 0.0;

for(i=0;i<(588 - Parmwind);i++){
N = 0;
KL = 0;
KR = 0;
a = Lower;
c = Upper;
b = Upper;

for(h=0;h<NPW;h++)  X[h] = 1.0;

if((InFile = fopen(argv[1], "r")) == NULL){
printf("\nCannot open file %s\n", argv[1]);
exit(0);
}
j = (float) i;
while(fscanf(InFile,"%f %lf", &Minutes, &Magnitude) != EOF)
if(Minutes >= j*1440.0 && Minutes < (j*1440.0 +
1440.0*(float)Parmwind)){
X[N] = Magnitude - Cutoff;
++N;
}

Ya = f(a, N, X); Yc = f(c, N, X);
if(Ya*Yc >= 0.0){
printf("\nNo root, or else even number of roots, in [a, c]\n");
exit(0);
}

k = 0;

while(++k < IL && c-a > CC){
b = a-Ya*(c-a)/(Yc-Ya);
Yb = f(b, N, X);
if(Ya*Yb < 0.0){
c = b; Yc = Yb;
KR = 0; KL = KL+1;
if(KL > 1) Ya = 0.5*Ya;
}
```

```
else{
a = b; Ya = Yb;
KL = 0; KR = KR+1;
if(KR > 1) Yc = 0.5*Yc;
}
}

dParmwind = (double) Parmwind;
dN = (double) N;
dD = (double) D;
ar = dN*dD/dParmwind;

HAZ[i][0] = b;
HAZ[i][1] = BV(b, N, X);
HAZ[i][2] = 1.0 - exp(-ar*exp(-HAZ[i][1]*pow((xm-Cutoff), b)));
HAZ[i][3] = (double) N;
fclose(InFile);
}

for(i=0;i<(588 - Parmwind);i++)
fprintf(OutFile, "%9.5lf %9.5lf %9.5lf %8.0lf\n",
                  HAZ[i][0], HAZ[i][1], HAZ[i][2], HAZ[i][3]);
}

double f(double q, int n, double *P){
int i;
double R, S1, S2, S3, m;
R = 0.0; S1 = 0.0; S2 = 0.0; S3 = 0.0;
m = (double) n;
for(i=0;i<n;i++){
S1 += log(P[i]);
S2 += pow(P[i], q);
S3 += pow(P[i], q)*log(P[i]);
}
R = (1.0/q) + (S1/m) - (S3/S2);
return (R);
}


double BV(double cee, int numb, double *Mag){
int i;
double beta, Sum, m;
m = (double) numb;
Sum = 0.0;
for(i=0;i<numb;i++) Sum += pow(Mag[i], cee);
beta = m/Sum;
return (beta);
}
```

E.8 : Listing of runtime.h header file (see Anderson and Anderson 1989)

```
/*****************************************************************/
/*                                                               */
/*  Included Macros       DIM1(pdata, col, type)                 */
/*                        DIM2(prow, row, col, type)             */
/*                        DIM3(pgrid, grid, row, col, type)      */
/*                                                               */
/*****************************************************************/

#define DIM1(pdata, col, type){\
pdata = (type *) calloc((col), sizeof(type));\
if(pdata == (type *) NULL){\
printf("No heap space for data\n");\
exit(0);\
}\}
```

```
#define DIM2(prow, row, col, type){\
register type *pdata;\
int h;\
pdata = (type *) calloc((row)*(col), sizeof(type));\
if(pdata == (type *) NULL){\
printf("No heap space for data\n");\
exit(0);\
}\
prow = (type **) calloc((row), sizeof(type *));\
if(prow == (type **) NULL){\
printf("No heap space for row pointers\n");\
exit(0);\
}\
for(h=0;h<(row);h++){\
prow[h] = pdata;\
pdata += (col);\
}\
}
#define DIM3(pgrid, grid, row, col, type){\
register type **prow;\
register type *pdata;\
int h;\
pdata = (type *) calloc((grid)*(row)*(col), sizeoftype;\
ifpdata == type *) NULL){\
printf("No heap space for data\n");\
exit(0);\
}\
prow = (type **) calloc((grid)*(row), sizeof(type*));\
if(prow == (type **) NULL){\
printf("No heap space for row pointers\n");\
exit(0);\
}\
pgrid = (type ***) calloc((grid), sizeof(type**));\
if(pgrid == (type ***) NULL){\
printf("No heap space for grid pointers\n");\
exit(0);\
}\
for(h=0;h<(grid)*(row);h++){\
prow[h] = pdata;\
pdata += (col);\
}\
for(h=0;h<(grid);h++){\
pgrid[h] = prow;\
prow += (row);\
}\
}
```

APPENDIX F

Fragment of the Data

In appendix E, several listings referred to "input files" with the format

YY MM DD hh mm LocX LocY LocZ Moment Energy

where YY, MM, DD, hh, mm, stands for the year, month, day, hour and minute of occurrence of an event and LocX, LocY, LocZ are the x, y and z coordinates of the hypocentre of the event. The remaining entries are self explanatory.

It must be emphasised that the above format - which contains all the information required for this project - is, nevertheless, a severely abridged version of the ordinary output of the ISS system.

For the benefit of readers unfamiliar with the "feel" of mining induced seismic data, the following fragment is offered.

Table F1 A fragment of mining-induced seismic data

YY	MM	DD	hh	mm	LocX	LocY	LocZ	Moment (Nm)	Energy (J)
92	7	8	0	58	28539	-43566	3543	1.700000e+10	1.490000e+05
92	7	8	1	0	26536	-45802	2848	4.560000e+11	7.030000e+06
92	7	8	2	44	27113	-43572	3043	1.970000e+11	1.930000e+07
92	7	8	3	12	28836	-41487	3235	2.690000e+11	1.100000e+07
92	7	8	3	14	28810	-41527	3269	7.490000e+10	8.510000e+05
92	7	8	4	46	28618	-42939	2091	6.400000e+09	7.150000e+04
92	7	8	5	17	28924	-32857	3107	2.120000e+12	2.930000e+09
92	7	8	5	37	28787	-42041	2399	9.170000e+09	7.180000e+04
92	7	8	6	11	26334	-45667	2633	2.630000e+11	2.300000e+06
92	7	8	6	49	30344	-37766	2320	5.160000e+10	1.390000e+05
92	7	8	6	59	32010	-35093	3390	4.480000e+11	5.770000e+07
92	7	8	7	13	29224	-39728	3412	1.090000e+10	8.250000e+04
92	7	8	7	32	28102	-42477	2318	2.440000e+12	9.480000e+07
92	7	8	7	37	27802	-41274	3075	8.510000e+10	7.670000e+06
92	7	8	8	41	28702	-39153	1982	1.250000e+12	1.250000e+07
92	7	8	9	29	31531	-33666	2388	1.410000e+12	7.370000e+07
92	7	8	10	33	29336	-39698	3309	2.170000e+12	2.020000e+08
92	7	8	10	34	29248	-39776	3450	6.170000e+09	1.200000e+05
92	7	8	11	48	28896	-38667	3162	1.560000e+10	5.620000e+04
92	7	8	13	18	27872	-40855	1984	4.440000e+10	5.380000e+05
92	7	8	13	38	28096	-42539	2408	2.350000e+10	7.350000e+05

APPENDIX G

Correlation between Seismicity in Adjacent Areas

Because of the importance of this topic in the current project, a summary of an ISS Report (Kijko, 1993) dealing specifically with this matter has been included as a separate appendix and not simply quoted in the refrences.

Table G1 X, Y coordinates of 4 analyzed clusters of seismic events.

CLUSTER #	X_{min} (km)	X_{max} (km)	Y_{min} (km)	Y_{max} (km)
1	7.7	8.6	- 4.3	- 3.6
2	7.3	7.7	- 4.8	- 4.3
3	7.0	7.7	- 4.2	- 3.7
4	8.3	8.7	- 3.4	- 2.8

Table G2 Maximum cross-correlation coefficients.

		Activity Rate Correlation			
Energy Correlation		*1*	*2*	*3*	*4*
	1	-	*0.82*	*0.89*	*0.77*
	2	*0.79*	-	*0.87*	*0.64*
	3	*0.91*	*0.88*	-	*0.75*
	4	*0.79*	*0.69*	*0.77*	-

REFERENCES

Aki, K. (1965). Maximum likelihood estimate of b in the formula $\log N = bM$ and its confidence limits. *Bull. Earthq. Res. Inst. Tokyo Univ.*, **43**, 237-239.

Aki, K., and Richards, P.G. (1980). *Quantitative Seismology, Theory and Methods*, Volume 1. W.H. Freeman and Company.

Anderson, P.L., and Anderson G.C. (1989). *Advanced C: Tips and Techniques.* Hayden Books

Angell, I.O., and Griffith, G. (1989). *High-resolution Computer Graphics Using FORTRAN 77.* Macmillan Education Ltd.

Bender, B. (1983). Maximum likelihood estimation of b values for magnitude grouped data. *Bull. Seism. Soc. Am.*, **73**, 831-851.

Cornell, C.A., and Winterstein, S.R. (1988). Temporal and magnitude dependence in earthquake recurrence models. *Bull. Seism. Soc. Am.*, **78**, 1522-1537.

Cosentino, P., Ficara, V., and Luzio, D. (1977). Truncated exponential frequency-magnitude relationship in the earthquake statistics. *Bull. Seism. Soc. Am.*, **67**, 1615-1623.

Cox, D.R., and Lewis, P.A.W. (1966). *The Statistical Analysis of Series of Events*, Methuen, London.

Davis, S.D., and Frohlich, C. (1991). Single-link cluster analysis, synthetic earthquake catalogues, and aftershock identification. *Geophys. J. Int.*, **104**, 289-306.

Eadie, W.T., Dryard, D., James, F.E., Roos, M., and Sadoulet, B. (1982). *Statistical Methods in Experimental Physics.* North-Holland Publishing Company.

Frohlich, C., and Davis, S.D. (1990). Single-link cluster analysis as a method to evaluate spatial and temporal properties of earthquake catalogues. *Geophys. J. Int.*, **100**, 19-32.

Johnson, N.L., and Kotz, S. (1970). *Continuous Univariate Distributions* - 1. *Distributions in Statistics.* John Wiley & Sons.

Kijko, A. (1993). Correlation between Seismicity in Adjacent Mining Areas. *Report ID: ISS/SR/8/VER1* ISS International Ltd.

Kijko, A., and Funk, C.W. (1993). Nonstationary Model for Seismic Event Occurrence in Mines. *Report ID: ISS/SR/6/VER1* ISS International Ltd.

Kijko, A., Funk, C.W., and Brink, AvZ. (1993). Identification of Anomalous Patterns in Time-dependent mine Seismicity. *Proc. 3rd Int. Symp. Rockbursts and Seismicity in Mines".*

Kijko, A., and Gibowicz, S.J. (1993). *Introduction to Mining Seismology,* Academic Press. In print.

Kijko, A., and Sellevoll, M.A. (1989). Estimation of earthquake hazard parameters from incomplete data files. Part I. Utilization of extreme and complete catalogs with different threshold magnitudes. *Bull. Seism. Soc. Am.*, **79**, 645-654.

Kijko, A., and Sellevoll, M.A. (1992). Estimation of earthquake hazard parameters from incomplete data files. Part II. Incorporation of magnitude heterogeneity. *Bull. Seism. Soc. Am.*, **82**, 120-134.

Main, I.G., Meredith, P.G., and Jones, C. (1989). A reinterpretation of the precursory seismic *b*-value anomaly from fracture mechanics. *Geophys. J.*, **96**, 131-138.

Matsumura, S. (1984). A one-parameter expression of seismicity patterns in space and time. *Bull. Seism. Soc. Am.*, **74**, 2559-2576.

McGillem, C.D., and Cooper, G.R. (1991). *Continuous and Discrete Signal and System Analysis.* Saunders College Publishing.

Mood, A.M., Graybill, F.A., and Boes, D.C. (1974). *Introduction to the Theory of Statistics.* McGraw-Hill.

Nakamura, S. (1993). *Applied Numerical Methods in C.* Prentice-Hall Int.

Reyners, M. (1981). Long- and intermediate-term seismic precursors to earthquakes - State of the art. In *Earthquake Prediction.* D.W. Simpson and P.G. Richards (eds), Maurice Ewing Series 4, 333-347. American Geophysical Union.

Shi, Y., and Bolt, B.A. (1982). The standard error of the magnitude-frequency *b* value. *Bull. Seism. Soc. Am.*, 72, 1677-1687.

Spottiswoode, S.M., and McGarr, A. (1975). Source parameters of tremors in a deep-level gold mine. *Bull. Seism.Soc. Am.*, 65, 93-112.

Stewart, R.D., and Spottiswoode, S.M. (1993). A technique for determining the seismic risk in deep-level mining. *Chamber of Mines Research Organisation* (COMRO), Johannesburg, South Africa.

Tsubokawa, I. (1969). On relation between duration of crustal movement and magnitude of earthquake expected. *J. Geod. Soc. Japan*, 15, 75-88 (in Japanese) *

Tsubokawa, I. (1973). On relation between duration of precursory geophysical phenomena and duration of crustal movement before earthquake. *J. Geod. Soc. Japan*, 19, 116-119. (in Japanese) *.

Utsu, T. (1965). A method for determining the value of *b* in the formula $\log n = a - bM$ showing the magnitude-frequency relation for earthquakes. *Geophys. Bull. Okkaido Univ.* 13, 99-103. (In Japanese; English abstract) *

Utsu, T. (1971). Aftershocks and earthquake statistics (III). *Journal of the Faculty of Science, Hokkaido University, Ser. VII, Geophysics, Vol. III*, *No.* 5, 1971.

Utsu, T. (1984). Estimation of parameters for recurrence models of earthquakes. *Bull. Earthq. Res. Inst. Univ. Tokyo,* 59, 53-66.

Woods, F.S. (1954). *Advanced Calculus.* Ginn and Company.

* In translation - Goldfields Information Services.

Author: Finnie Gerard John.
Name of thesis: Time-dependent seismic hazard in mining.

PUBLISHER:
University of the Witwatersrand, Johannesburg
©2015

LEGALNOTICES:

Copyright Notice: All materials on the University of the Witwatersrand, Johannesburg Library website are protected by South African copyright law and may not be distributed, transmitted, displayed or otherwise published in any format, without the prior written permission of the copyright owner.

Disclaimer and Terms of Use: Provided that you maintain all copyright and other notices contained therein, you may download material (one machine readable copy and one print copy per page)for your personal and/or educational non-commercial use only.

The University of the Witwatersrand, Johannesburg, is not responsible for any errors or omissions and excludes any and all liability for any errors in or omissions from the information on the Library website.